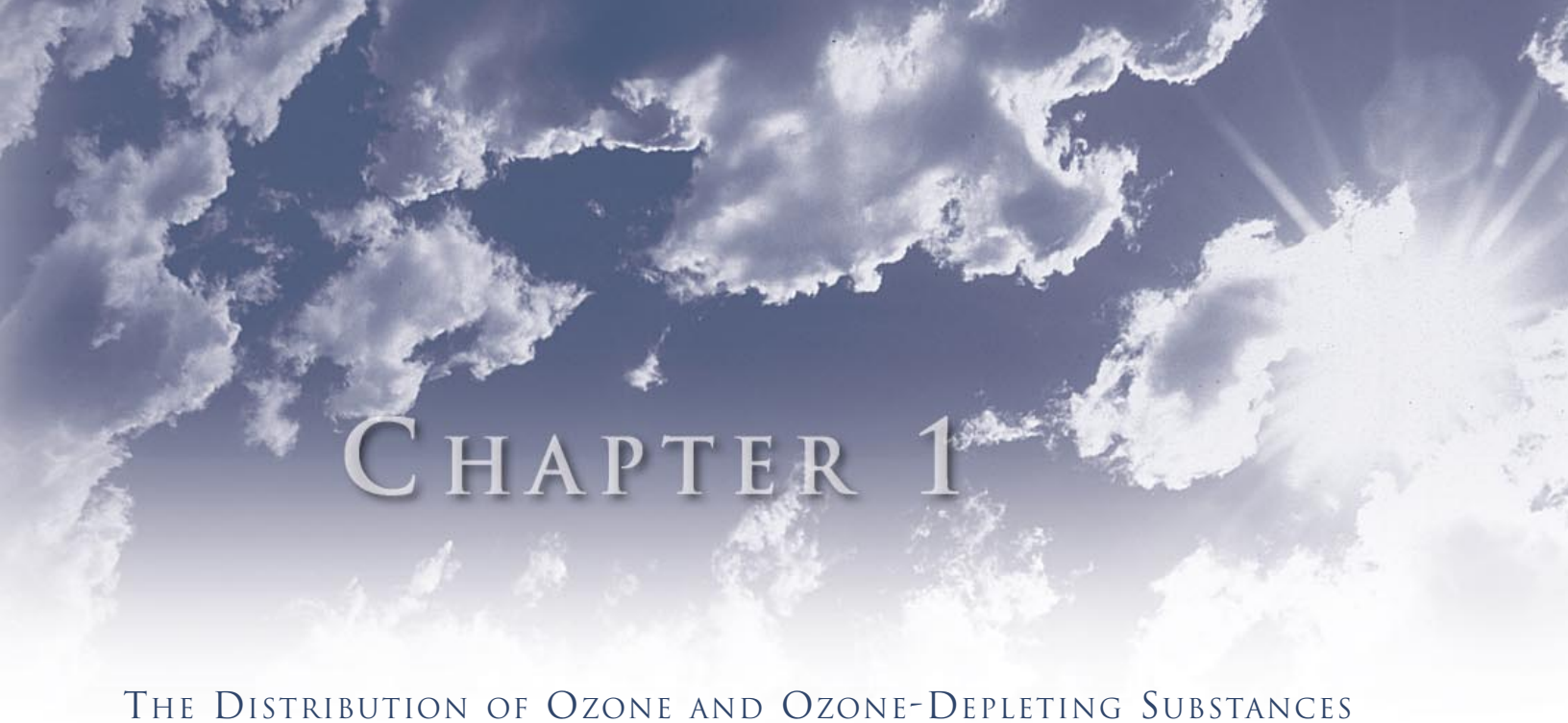

Chapter 1

The Distribution of Ozone and Ozone-Depleting Substances in the Atmosphere and Observed Changes

1.1 Global Ozone Measurement and Monitoring

Ozone (O_3), an allotrope of ordinary oxygen (O_2), is the most important trace constituent in the stratosphere. Although it is present in relative concentrations of no more than a few parts per million, it is such an efficient absorber of ultraviolet radiation that it is the largest source of heat in the atmosphere at altitudes between about 10 and 50 km. UV absorption by ozone causes the temperature inversion that is responsible for the existence of the stratosphere. Ozone is also an important radiator, with strong emission bands in the 9.6 mm infrared region. In the UV-B region (290–315 nm) it absorbs with an efficiency that increases exponentially with decreasing wavelength, and so strongly that at 290 nm the radiation at the ground is reduced by more than a factor of 10^4 from that above the ozone layer (see Chapter 4). This strong variation of absorption efficiency with wavelength in the UV-B region is the basis of the Dobson and Brewer operational methods of measuring ozone.

Ozone is the main source of the highly reactive OH radical, which causes the removal of many organic molecules from the atmosphere. In the troposphere, it is also a pollutant, which means that its natural concentration is augmented by anthropogenic sources. Because its extra oxygen bond can be easily broken, ozone is a strong oxidant that is both corrosive to materials and toxic to plants and animals. A principal component of urban smog, it is produced in and downwind of urban centres by photochemical reactions involving volatile organic hydrocarbons (VOCs) and oxides of nitrogen (NO_x) (see Chapter 3). Intrusions of stratospheric air are also a significant source of ozone in the troposphere (see Chapter 2). Globally, the distribution and climatology of tropospheric ozone appear to be highly variable and have not yet been well established by comprehensive measurements. Although this is a very important area of current research, this document will deal primarily with the state of current knowledge of ozone in the stratosphere.

Regular measurments of the ozone content of the atmosphere were initiated in the early 1920s by G.M.B. Dobson using spectrographic instruments. He built his first version of what is now known as the Dobson ozone spectrophotometer in 1927. It makes precise measurements of the relative intensities of sunlight at pairs of wavelengths in the UV spectrum; the total ozone column[1] is deduced from these measurements and the known absorption coefficients of ozone at the wavelengths of measurement. Canada acquired a Dobson in 1948. Until the 1950s there were only about 20 regularly operating stations in the world, most of which were located in the northern hemisphere. Some of these had already interrupted their measurement programs in the late 1950s. At this time the reason for studying ozone was the hope that research into stratospheric motion, of which ozone was a useful tracer, would lead to improved models for forecasting the weather. It is for this reason that we have such a comprehensive data base of ozone measurements for the 1960s and 1970s, well before ozone depletion became a scientific issue. Systematic ozone observations using common observational methods and calibration procedures laid out by the International

1 Equivalent thickness of the ozone layer, expressed as a vertical column of pure ozone. The standard unit is the Dobson Unit, equal to 10^{-5}m at 0˚C and sea level pressure (STP). The global average of total ozone is approximately 300 DU, equivalent to a thickness of 3 mm.

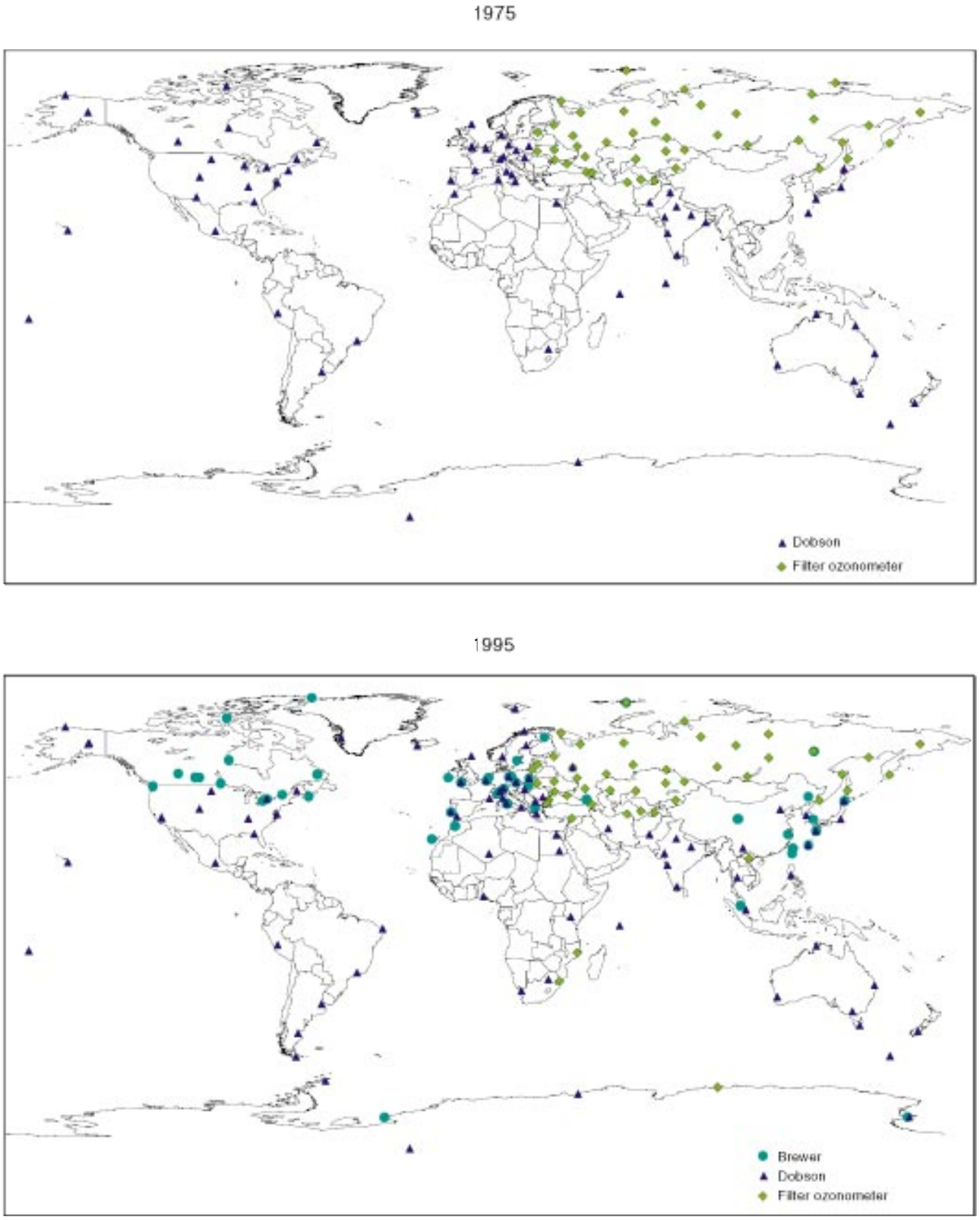

Figure 1.1 Geographical distribution of ground-based ozone measurement stations in 1975 and 1995.

Ozone Commission in collaboration with the World Meteorological Organization (WMO) were started in preparation for the International Geophysical Year (1957–1958). These standard procedures formed the basis of the Global Ozone Observing System, which presently has more than 160 continuously operating stations. Three main types of instruments are used for routine total ozone observations: Dobson and Brewer spectrophotometers that can measure total ozone with up to 1% accuracy [e.g., Kerr et al.1988] and the less accurate M-83 and M-124 filter ozonometers [e.g., Bojkov et. al. 1994]. Figure 1.1 shows the geographical distribution of stations. The World Ozone and UV Radiation Data Centre, the international repository for all ground-based measurements of ozone, is housed at Environment Canada in Toronto.

A relatively small number of stations make regular measurements of the vertical profile of ozone concentration using balloon-borne ozonesondes. Two principal types of ozonesonde exist: the Brewer-Mast [Brewer and Milford 1960] and the ECC [Komhyr 1969]. Both types measure the ozone concentration *in situ*, via its reaction with an aqueous solution of potassium iodide. The technique is very sensitive and can give very fine vertical resolution. It is also capable of excellent accuracy, but sensitivity to contamination as well as errors arising from improper handling or occasional mechanical defects in the sonde itself render it less reliable than optical methods. For this reason sonde data are compared, whenever possible, with Brewer or Dobson total ozone measurements.

Only a few stations have been making regular measurements since before the 1980s. Since ozone loss now appears to have started sometime between 1970 and 1980, their records are of particular significance. The time series of ozone soundings from these stations represent some of the longest records of ozone measurement that exist, as well as the only time series of measurements in the free troposphere and the most precise vertically resolved measurements in the lower stratosphere. The stations with important long-term records are: Hohenpeissenberg and Lindenberg (Germany), Payerne (Switzerland), Uccle (Belgium), Boulder, Wallops Island (contiguous United States), Barrow (Alaska), Hilo (Hawaii), Resolute, Churchill, Goose Bay, and Edmonton (Canada), Tateno and Sapporo (Japan), and the South Pole and Syowa in Antarctica. A much larger number of stations have started making soundings more recently, and a number of other stations have important but intermittent records. Regular ozone soundings have been made since 1966 in Canada and are currently made weekly at six stations. Additional flights are made during times of special interest, like the Arctic spring.

Umkehr observations are made by using an ultraviolet spectrophotometer to measure the intensity of light from the zenith sky at various wavelengths over a range of solar zenith angles between 60° and 90°. As the sun sets (or rises) the mean scattering height of radiation changes as a result of the attenuation of the direct and scattered radiation by ozone absorption and Rayleigh scattering. Since both ozone absorption and Rayleigh attenuation increase toward shorter wavelengths, the mean scattering height moves upward more rapidly as a function of the solar zenith angle for shorter wavelengths than it does for longer wavelengths. The short-wavelength light, which is scattered higher in the atmosphere, travels along a path which passes, on average, through less ozone. The variation of the intensity of light as a function of wavelength and zenith angle can therefore be used to determine the vertical profile of ozone, provided that the ozone distribution remains constant throughout the period.

The vertical resolution of the Umkehr method is about two scale heights (5–10 km) in the stratosphere [Mateer and Dutsch 1964; Mateer and Deluisi 1992; McElroy and Kerr 1995]. The Umkehr method is relatively insensitive to the distribution of ozone in the lower atmosphere (0 to 15 km). Figure 1.2 [McElroy and Kerr 1995] shows the performance of the Brewer Umkehr as compared with the mean profile inferred from measurements made by lidar, ozonesondes, and a microwave radiometer. It can be seen that the Umkehr retrieval performs very well in the 20–40 km altitude range and provides useful information to 45 or 50 km.

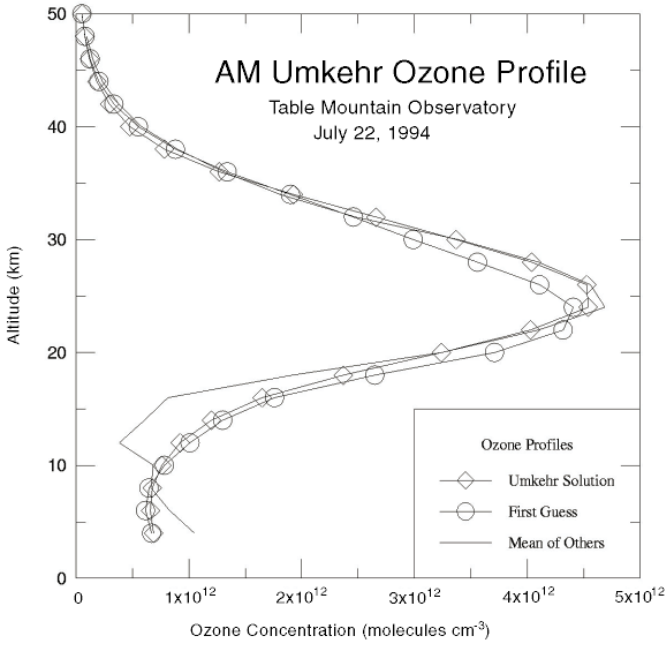

Figure 1.2 Comparison of an Umkehr-derived profile with the mean of other profile measurements (two lidars, one sonde, and one microwave) [McElroy and Kerr, 1995].

Umkehr observations have been made since the effect was first studied by Götz [Götz et al. 1934] in the 1920s, and Umkehr observations are included as a regular part of the automated observing schedules of the Brewer spectrophotometer. Analysis of these data for trends in the vertical distribution of ozone at higher altitudes is complex, and although such studies have been published for Dobson observations [Mateer and Dutsch 1964; Deluisi et al. 1989; WMO 1994] up to now, much less has been done with data from the newer Brewer instruments [Hahn et al. 1995; McElroy et al. 1997].

Dobson ozone spectrophotometers were installed at five sites in Canada between 1957 and 1964. These were replaced in the mid-1980s by the automated Brewer ozone spectrophotometer, developed by scientists at Environment Canada. The Brewer compares the intensities of five UV-B wavelengths in order to better correct for the influence of absorbers other than ozone. It is now in use at some 90 sites worldwide. Brewer instruments have been installed recently at seven additional sites in Canada (Table 1; Figure 1.3). Data from the Brewer network are delivered in quasi-real time to the operational weather forecast centre for use in producing the daily ozone and UV Index forecast. Modified versions of the Brewer spectrophotometer are also being used to monitor NO_2 column amounts at several sites and to make spectrally resolved UV-B measurements at all Canadian sites. With its great geographical area, Canada has one of the largest ground-based ozone measurement networks in the world.

Table 1: Canadian Ground-Based Ozone Measurement Sites

Station	Total Ozone	Other Instrumentation
Alert	Brewer (1989)	Ozonesondes (1987)
Churchill	Brewer (Dobson 1964)	Ozonesondes (1973)
Edmonton	Brewer (Dobson 1957)	Ozonesondes (1970)
Eureka	Brewer (1992)	Ozonesondes, lidars, FTIR spectrometers Fabry-Perot spectrometers, radiometers
Goose Bay	Brewer (Dobson 1962)	Ozonesondes (1969)
Halifax	Brewer (1992)	
Montreal	Brewer (1993)	
Resolute	Brewer (Dobson 1957)	Ozonesondes (1966)
Saskatoon	Brewer (1988)	
Saturna	Brewer (1990)	
Toronto	Brewer (Dobson 1960)	Lidar, 1991. [ISTS]
Regina	Brewer (1994)	
Winnipeg	Brewer (1992)	

Date indicates the start of regular observations. All sites are operated by Environment Canada, except that of the Toronto lidar of the Institute for Space and Terrestrial Science (ISTS), which also operates the ozone lidar at Eureka.

Figure 1.3 Canadian ground-based ozone measurement stations in 1997.

The Network for the Detection of Stratospheric Change (NDSC) is a set of high-quality, ground-based, remote-sounding research stations for observing and understanding the physical and chemical state of the stratosphere. Ozone and key ozone-related chemical compounds and parameters are targeted for measurement. The NDSC is a major component of the international upper atmosphere research effort and has been endorsed by national and international scientific agencies, including the International Ozone Commission, the United Nations Environment Programme (UNEP), and the WMO. Following five years of planning, instrument design, and implementation, the NDSC began network operations in January 1991. The goals of the network are:

1 To make observations so that changes in the physical and chemical state of the stratosphere can be determined and understood and, in particular, so that changes in the ozone layer can be detected and their causes identified as early as possible.
2 To provide an independent calibration of satellite sensors of the atmosphere.
3 To obtain data that can be used to test and improve multi-dimensional stratospheric chemical and dynamical models.

A high-Arctic stratospheric ozone observatory was built by Environment Canada in 1992 near the Eureka weather station on Ellesmere Island. This observatory is a centre for atmospheric research in the Arctic and a primary component of the NDSC. It is used by researchers from Canadian Universities, Japan, and the USA as well as Environment Canada. Observations are carried out with two lidar systems, one designed for obtaining vertical profiles of ozone and temperature [Donovan et al. 1996] and the other for determining the vertical structure of aerosols from volcanic eruptions or in the form of polar stratospheric clouds and Arctic haze. Ozone is being monitored also by means of a modified Brewer spectrophotometer and ozonesondes launched from the Eureka weather

Figure 1.4 The Eureka NDSC High-Arctic Stratospheric Ozone Observatory. (Photo by Luc Sarrazin and Greg Sorensen.)

station. Fourier Transform Infra-Red (FTIR) spectrometers are used to determine the column amounts of several atmospheric gases of importance in the ozone chemistry, such as hydrofluoric and hydrochloric acid [Donovan et al. 1997].

Since 1970 satellites have provided a global picture of total ozone and (to a lesser extent) its vertical distribution. The Backscatter Ultraviolet (BUV) instrument, launched on board the Nimbus 4 satellite in April 1970 is a source for several years of early total ozone data [Stolarski et al. 1997]. Since 1978 the Total Ozone Mapping Spectrometer (TOMS) instruments on Nimbus 7, Meteor 3 [Herman and Larko 1994], and recently on Earth Probe and ADEOS have provided a record of high-resolution daily global total ozone data that now extends over more than 17 years. Long-term records of ozone observations are available from several other satellite instruments: the Solar Backscatter Ultraviolet (SBUV) (1979) and SBUV/2 (several since 1984), the Stratospheric Aerosol and Gas Experiment (SAGE) and SAGE II (1979 and 1984), and the Tiros Operational Vertical Sounder (TOVS) instruments, as well as several instruments on the Upper Atmosphere Research Satellite (UARS). More recently (1996) the Global Ozone Monitoring Experiment (GOME) on the European ERS-2 platform has begun making both global total ozone and profile measurements. Early space-based ozone measurements often compared poorly with ground-based data. However, extensive intercomparison with ground-based and other space-based instruments and careful work with instrument characterization have improved data reduction algorithms to the point where space-based measurements of total ozone are now reported to be compatible with those of the best-calibrated ground-based stations [McPeters and Labow 1996].

Canada participates in space-based monitoring of ozone through scientific and technical collaboration with other countries and cooperative agreements on data and cost sharing with meteorological and space agencies in the United States and Europe. The Canadian OSIRIS ozone spectrometer, due to be launched aboard the Swedish satellite ODIN in 1998, is one example of such collaboration. Canada has also shared some of the cost of the European ENVISAT platform (to be launched in 1999), which contains three instruments for measuring ozone and related chemical species. In addition, several Canadian instruments to study the chemistry and dynamics of ozone are proposed as part of the Canadian Space Agency's Long-Term Space Plan III.

Measurements made *in situ*, by large-payload high-altitude balloons and more recently by high-altitude aircraft, while not usually suitable for the monitoring activities described above, have played and continue to play a very important role in improving our understanding of the detailed chemistry of stratospheric ozone. The advantages of these platforms are that a large number of simultaneous measurements may be made, since many different instruments may be accomodated, and that direct, *in situ*, rather than remote sensing techniques may be used. Such measurements provide data that are directly comparable to outputs from photochemical models of the ozone layer and that are essential for their verification. A series of campaigns with the NASA ER-2 aircraft provided dramatic confirmation of the hypothesis that chlorine-catalyzed chemistry was responsible for the Antarctic ozone hole by demonstrating the anticorrelation of ClO and ozone during the hole's development [Anderson et al. 1989; Brune et al. 1989]. The goal of this program is to measure all of the chemical species that are important in controlling the ozone budget in the stratosphere, and their sources and sinks, and to make measurements of sufficient precision to understand and separate the roles of chemistry and transport. Recent campaigns have concentrated on midlatitude chemistry and that of the Arctic [Brune et al. 1990; other references within].

Canada has participated in a number of balloon campaigns [Evans et al., 1977, 1982, 1985; Hilsenrath et al. 1986] and participates in the ER-2 program through its contribution of a UV/visible spectrometer to make spectrally resolved absolute intensity measurements of solar radiation at photochemically active wavelengths and to measure ozone above the aircraft. The instrument has made more than 100 flights to date [McElroy 1995; McElroy et al. 1995].

Data assimilation is a statistical technique that is an essential feature of any modern numerical weather prediction system, and it is now being applied to ozone observations in the stratosphere by several groups worldwide [Fisher and

Lary 1995; Levelt et al. 1996]. The goal in data assimilation is to produce an optimal estimate of the value of an atmospheric state variable (such as ozone concentration) by combining observations, weighted inversely by their estimated error covariances, with prior estimates of that variable, weighted by their estimated error covariances. The prior estimates contain information from previous observations, from other measurements, or from measurements of related quantities (e.g., temperature or potential vorticity). This information is carried in an atmospheric model that expresses the physical, dynamical, and chemical relationships between these sources of prior information and the target variable. This is a powerful technique that can interpolate with great success in areas where data are sparse and correct (or highlight) both measurement and model deficiencies or inconsistencies. Both models and methods for minimizing the total error of estimation are increasing rapidly in sophistication.

Middle atmosphere modelling and data assimilation are also major research activities in Canada. The development of data assimilation algorithms for the instruments described above is underway in a collaborative effort between Environment Canada and several Canadian universities. Ozone and wind data will be assimilated via the Middle Atmosphere Model (CMAM), as well as the operational global forecast model [Tarasick et al. 1996a]. Similar ozone data assimilation research programs are underway in Europe, the U.S., and Australia. Increased knowledge of ozone circulation and dynamics is expected to lead to better understanding of stratospheric ozone variability and change (see Chapter 2). Moreover, because ozone is the major chemical and radiative constituent of the middle atmosphere, its inclusion in models may also lead to improvements in climate modelling for global change issues and in forecast skill for weather models, particularly in the medium and longer ranges.

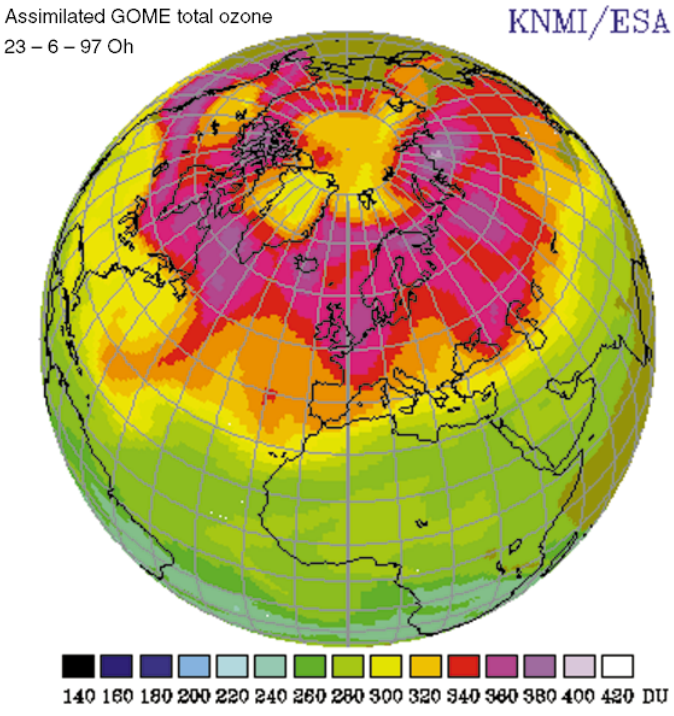

Figure 1.5 GOME data assimilation. (Royal Netherlands Meteorological Institute, KNMI)

1.2 Distribution, Climatology, and Natural Variation

1.2.1 Total Ozone Distribution

The main features of the global total ozone distribution were discovered during the first years of regular observations in the 1920s [Dobson et al. 1926, 1929, 1930]. The most important feature is a strong latitudinal gradient of total ozone, with lower values over the equator and tropics and higher values over middle and high latitudes (Figure 1.6). This gradient has a well-pronounced annual cycle, reaching a maximum in spring and a minimum in fall. The annual cycle in total ozone at a given point thus has an amplitude that is a function of latitude, with maximum amplitudes found at about 60° north and south latitude. In the tropics seasonal variations are small, with ozone maxima in summer; in the equatorial region there are essentially no seasonal variations.

The explanation for this behaviour, also deduced by Dobson and confirmed by Brewer [1949] from aircraft measurements of water vapour, is that the high values at extra-tropical latitudes are a result of transport from the tropical source region. Ozone is formed, primarily in the tropics at altitudes above about 30 km, via the action of ultraviolet light from the sun upon molecular oxygen. While the highest relative concentrations are found here, the more moderate values of 1–2 ppmv found at about 15 km actually make a much greater contribution to the total column ozone, because the density of the atmosphere is greater by an order of magnitude at the lower altitude. Mixing ratios in the lower stratosphere are higher at midlatitudes and toward the poles (Figure 1.7). This latitudinal distribution is made possible by the relatively long lifetime (months to years) of ozone in the lower stratosphere, and the Brewer-Dobson circulation (see Chapter 2) that transports stratospheric ozone from the tropics toward the poles and downwards at high latitudes. This circulation is both strongest and most variable in winter, and the highest total column amounts and the most variability are found in the winter stratosphere below 20 km.

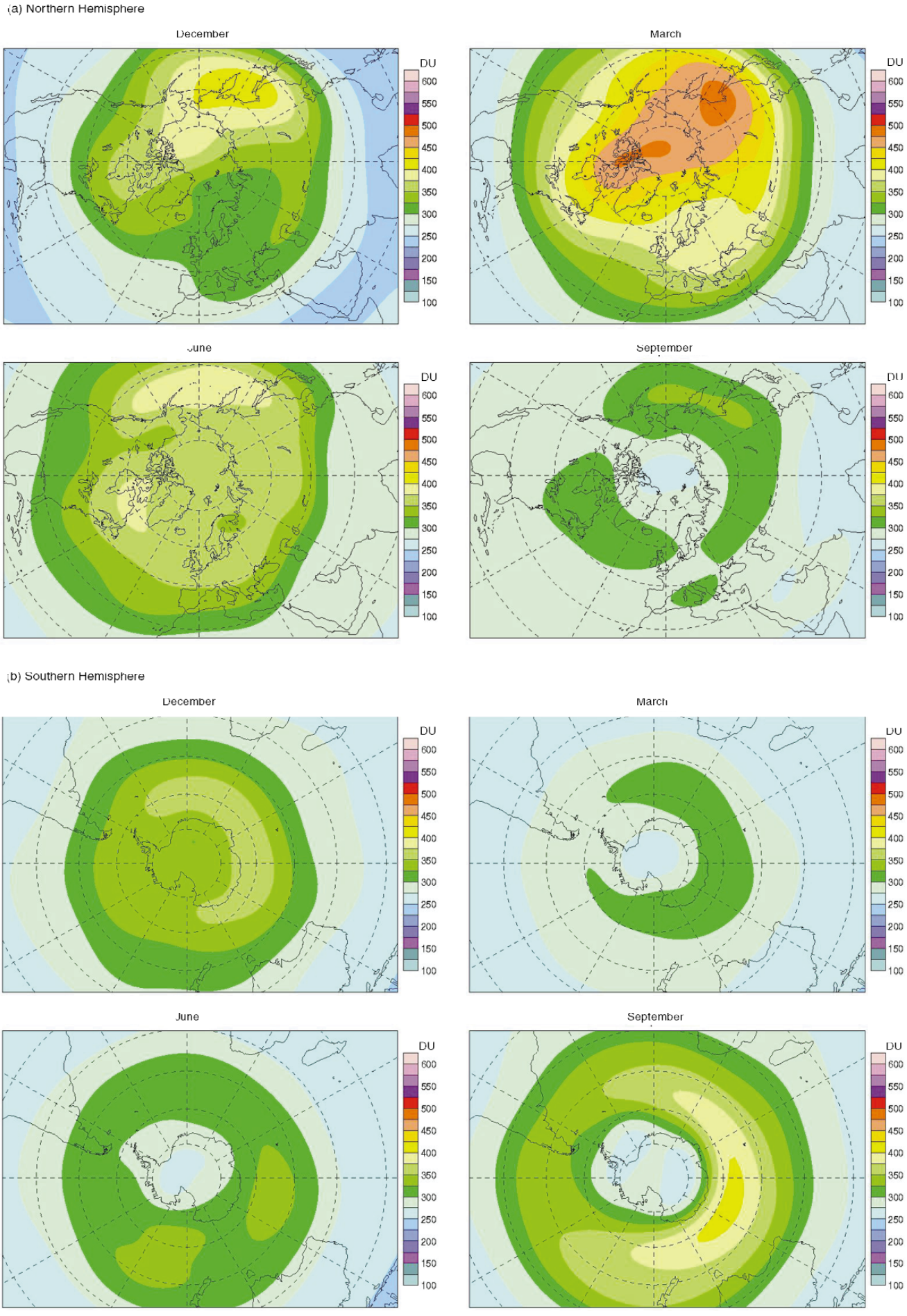

Figure 1.6 Global total ozone for the northern and southern hemispheres. (a) Northern hemisphere: average values for the period 1979–1988. (b) Southern hemisphere: average values for the period 1979–1988, except for the Antarctic where the period is 1960–1980.

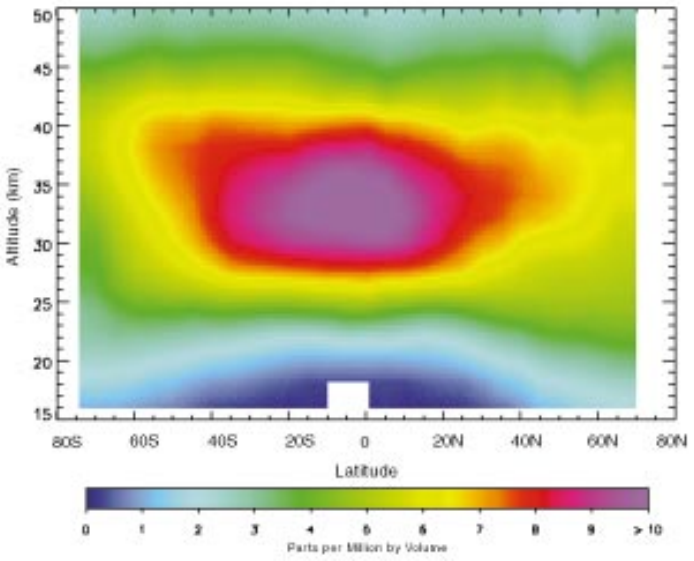

Figure 1.7 Average values of ozone mixing ratio as a function of altitude and latitude for March 1990. Data from SAGE II.

Expansion of the global ozone network during and after the International Geophysical Year (1957–1958) made it possible to analyse ozone climatology and to find longitudinal features in the ozone distribution such as the spring ozone maximum over the Canadian Arctic [London et al. 1976]. The global total ozone climatology has also been deduced from satellite data [e.g., Bowman and Krueger 1985]. More recently, Randel and Wu [1995] prepared a detailed atlas of total ozone, its variability and its vertical distribution, using SBUV and SBUV/2 data for the period 1978–1994.

Ozone variability also depends on season and latitude. It is lower in equatorial regions and over the tropics and higher over middle and high latitudes, especially in winter and spring. Standard deviations from the annual cycle for daily means are about 4–5% in low latitudes, and, over middle and high latitudes, vary from 7–8% in fall to 12–15% in late winter and early spring..

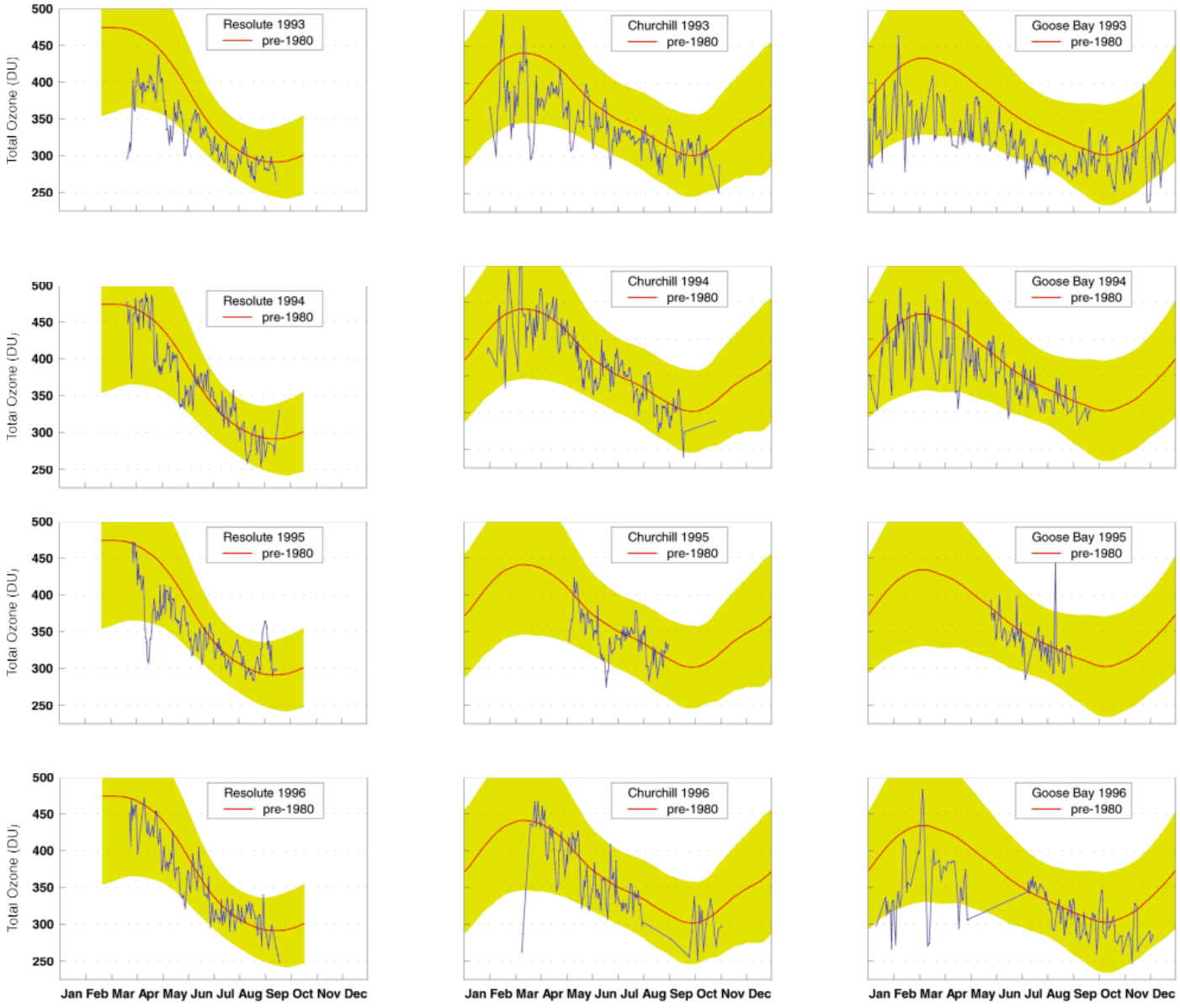

Figure 1.8 shows daily averages of total column ozone at five Canadian stations. Only direct-sun observations (the most reliable) have been used. Both the range of variation of the ozone column (which is greater in winter) and the seasonal cycle are evident. The data are plotted against the average of all values measured prior to 1980, indicated by the (smoothed) curve. Here, as elsewhere, we use the pre-1980 period as a baseline for the "natural" atmosphere. The shaded area shows the 2σ range of variation for this period (95% of observations made prior to 1980 fall within this range). In the top row of figures one may see clearly the record low ozone levels observed at all Canadian stations in early 1993 [Kerr et al. 1993].

The total ozone distribution over Canada is typical of that for the northern middle and high latitudes: the annual cycle has its maximum in March and its minimum in October, and spring ozone values in high latitudes are higher than over middle latitudes. Figure 1.9 shows the average total ozone distribution over Canada for the period 1979–1988. The maps were prepared using TOMS satellite data, with the addition of Dobson and Brewer moon observations for the polar night areas [Fioletov 1993]. The spring ozone maximum is evident in Figure 1.9. Over the Canadian Arctic station at Resolute, total ozone can reach values as high as those observed anywhere else on the globe (~600 DU). In September the latitudinal gradient of ozone is much smaller.

1.2.2 Vertical Ozone Distribution

The vertical profile of ozone can be expressed either by the mixing ratio, usually in parts per million or billion by volume, or by the concentration, typically in molecules per cubic centimeter or in Dobson units per kilometre, or by the partial pressure of ozone, usually in nanobars (10^{-6} hPa). The partial pressure and product of concentration and absolute temperature are proportional.

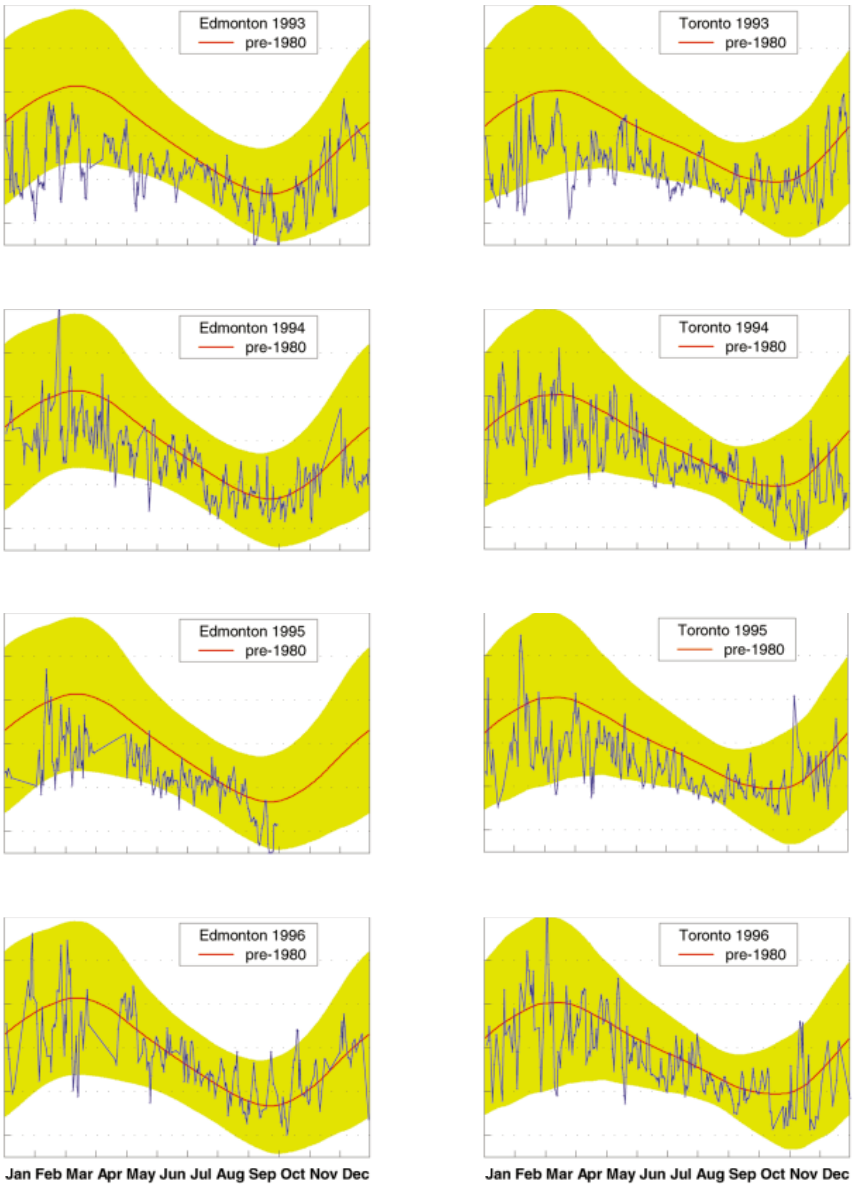

Figure 1.8 Daily observations of total column ozone at five Canadian stations, 1993–1996. The 60-day (smoothed) average of all observations made prior to 1980 is also shown. Spring values are generally lower than the pre-1980 average. The smoothing is performed with a 60-day full-width, half-maximum, triangular filter, similar to that described in Section 1.3.1.

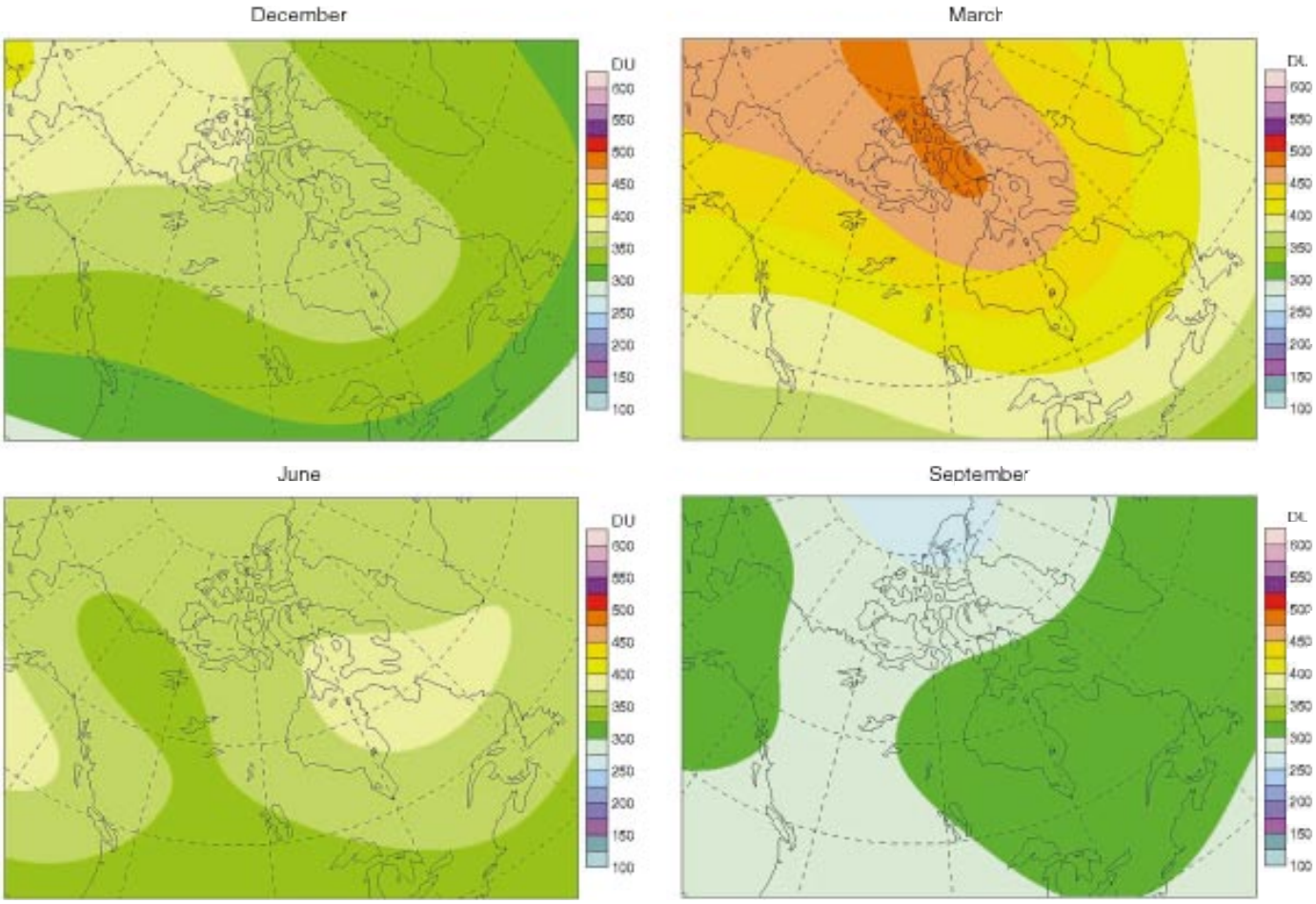

Figure 1.9 Average total ozone distribution over Canada for the period 1979–1988 for (a) December, (b) March, (c) June, (d) September.

Figure 1.10 shows typical spring and fall ozone vertical profiles for Edmonton (53°N) and Resolute (78°N), along with the corresponding temperature profiles. The ozone mixing ratio is relatively constant in the troposphere, so that the ozone concentration (partial pressure) falls with increasing altitude until the tropopause (indicated by the minimum in temperature) is reached. Ozone concentration increases rapidly with altitude in the lower stratosphere, to a maximum near 100 hPa. The maximum at Resolute is larger and occurs at a slightly lower altitude.

The March profiles show strongly layered structures known as ozone laminae (see Chapter 2).

In the summer and fall the maxima are much smaller and occur at higher altitudes (because the tropopause is also higher). Figure 1.11 shows the average vertical distribution of ozone concentration for these same sites as a function of time of year.

1.2.3 Natural Ozone Variations

As Figure 1.8 indicates, ozone concentrations are highly variable on time scales of a few days or more. Day-to-day fluctuations in total ozone, especially over middle and high latitudes, can be quite large, in some cases 100 DU or more. These variations are clearly due to atmospheric dynamics. The stratosphere rides on top of the troposphere and is necessarily greatly influenced by pressure and temperature variations (i.e., synoptic-scale weather systems) in that more massive region of the atmosphere. The ozone laminae in Figure 1.10 are evidence of large-scale horizontal transport, while the total ozone variations are most strongly correlated with tropopause height.

Examination of longer time series reveals, in addition to the annual cycle, longer-term persistent variability from several sources [e.g., Angell and Korshover 1973]. The quasi-biennial oscillation (QBO) in ozone amounts is apparently

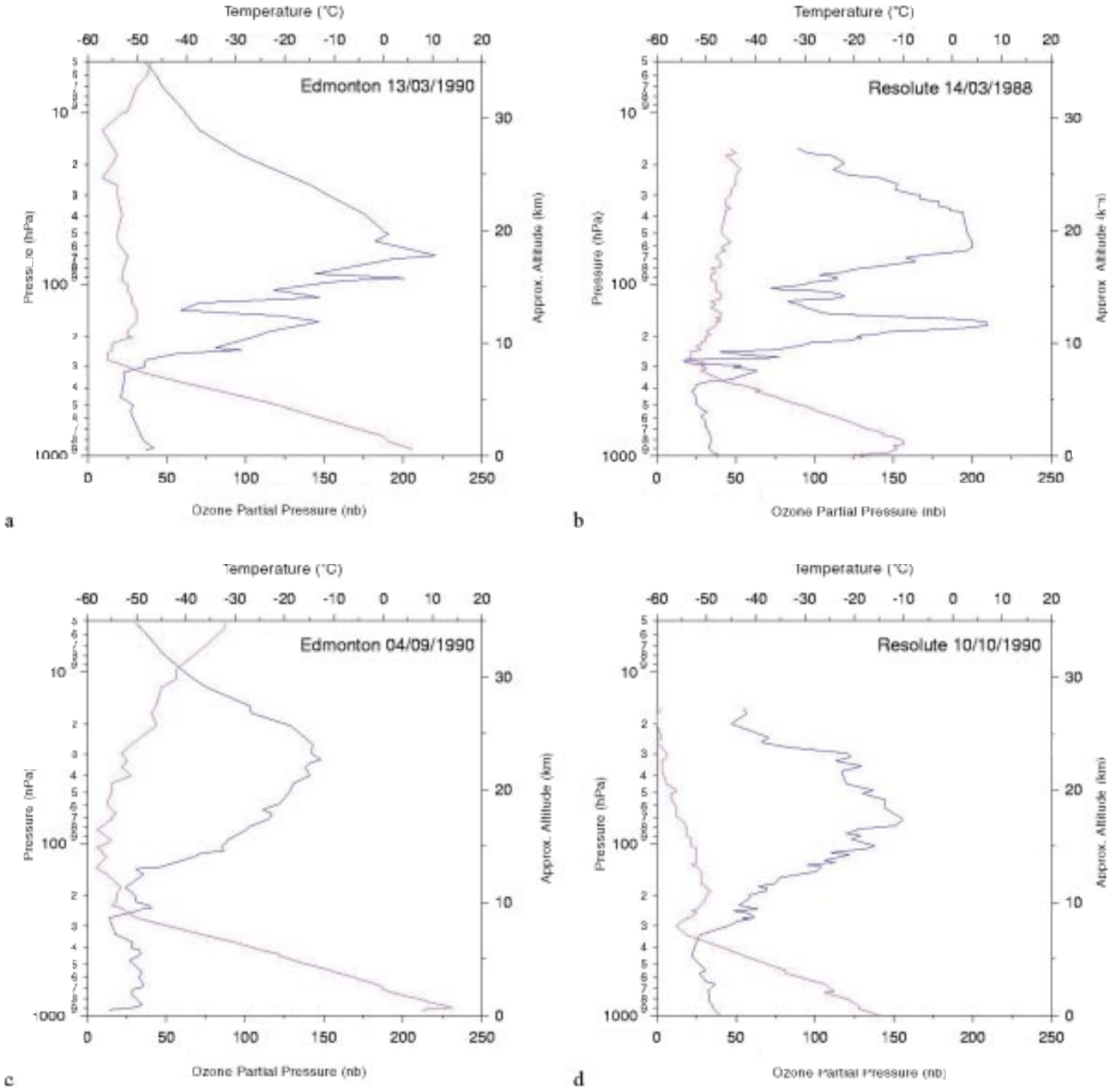

Figure 1.10 Vertical profiles of ozone partial pressure and temperature over (a) Edmonton, 13 March 1990, (b) Resolute, 14 March 1988, (c) Edmonton, 4 September 1990, and (d) Resolute, 10 October 1990.

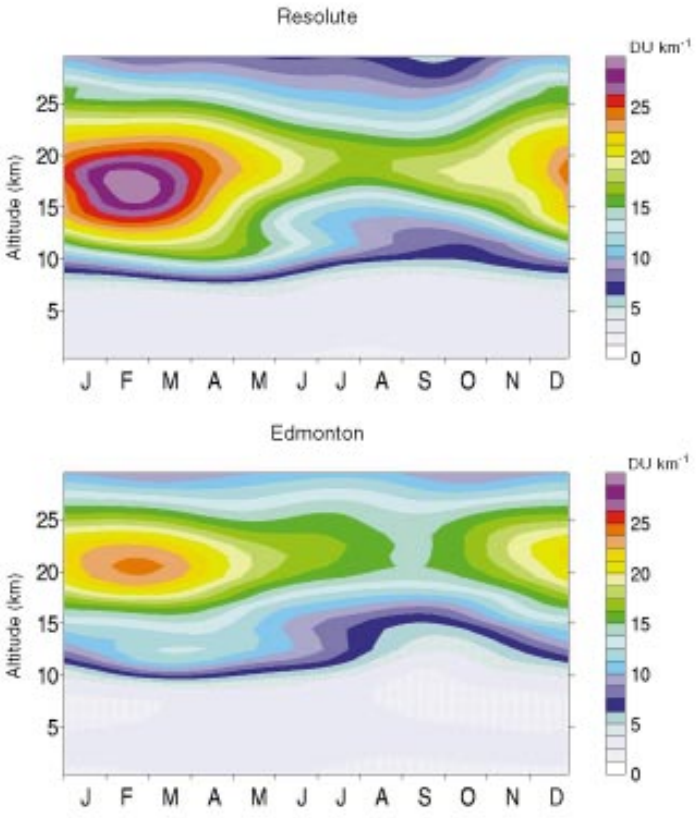

Figure 1.11 Annual variation of ozone density (in DU km^{-1}, based on pre-1988 long-term means) as a function of altitude for (a) Resolute Bay (78°N), (b) Edmonton (53°N).

caused by changes in the rate of meridional transport of ozone, induced by the quasi-biennial oscillation of the equatorial stratospheric wind. The period of the ozone QBO is about 27–28 months, although it may vary from 20 to 30 months. This is the dominant fluctuation in ozone after the annual cycle at low latitudes; its phase at middle and high latitudes is opposite to that in the tropics. The border between the two regimes is located between 10° and 15° in both hemispheres [Bowman 1989; Hamilton 1989; Chandra and Stolarski 1991; Hasebe 1994]. The amplitude of the QBO signal in the extraequitorial ozone record depends on the season [e.g., Randel and Cobb 1994, Yang and Tung 1994, Bojkov and Fioletov 1995]. It is usually in the 2–4% range [Hasebe 1983; Lait et al. 1989; Gray and Ruth 1993], although it can probably be higher in winter at high latitudes [e.g., Yang and Tung 1994].

The 11-year solar cycle causes the ozone production rate to vary with variations of solar activity. Although the variation in total solar output over the cycle is only about 1%, the change in output in the UV region is several times greater. The amplitude of the effect in total ozone is 1–2% [WMO 1989; Chandra and McPeters 1994, Huang and Brasseur 1993; Chandra 1991; Reinsel et al, 1987] and 5–7% in the upper stratosphere [Chandra and McPeters 1994].

A number of studies [Zerefos et al. 1992, Shiotani and Hasebe 1994; Randel and Cobb 1994] have found a significant El Niño Southern Oscillation (ENSO) signal in equatorial and tropical total ozone, with a characteristic time scale of about four years. Shiotani [1992] has shown a longitudinal difference in the ENSO signal over the equator: during El Niño events there are positive anomalies over the western Pacific and negative anomalies over the eastern Pacific. The anomaly pattern is reversed during La Niña events. In addition, zonal mean values for ozone in the equatorial region are smaller during El Niño events than in La Niña events. There is some evidence that an ENSO-related signal can be seen at extratropical latitudes [e.g., Randel and Cobb 1994], primarily over the Pacific, where the amplitude of the signal can be as much as 6% during strong ENSO events.

1.3 Trends in Total Ozone and its Vertical Distribution

1.3.1 Long-Term Ozone Changes

Since the mid-1980s substantial changes in the ozone layer have been detected. The discovery of the ozone hole in Antarctica [Farman et al. 1985] was the first unequivocal evidence of stratospheric ozone depletion. At that time total ozone levels in spring over Antarctica had dropped to 200 DU from the 300–350 DU levels prevailing in the 1960s and 1970s. Since that time, the hole has become, in general, deeper and wider each year. In the 1990s minimum ozone values of 110–120 DU were seen in Antarctica almost every year, and the total area with spring ozone values below 220 DU exceeded 20 million km^2. Total ozone values less than 100 DU were measured in both 1993 and 1994, with the record low value of 88 DU measured on September 28, 1994. In 1996 a minimum ozone value of 111 DU was recorded, while the area of the hole was almost as large as in the peak year of 1993 [NASA 1996]. Ozonesonde data have shown total destruction (>99%) of ozone from 14 to 19 km during ozone hole episodes in recent years [WMO 1994].

Figure 1.12 shows the mean latitude-time cross-section for the periods 1964–1980 and 1984–1993 [Bojkov and Fioletov 1995]. The hemispheric differences in the ozone distribution are clearly visible in the winter-spring months: in both time periods there is 50–75 DU less ozone at 60°S in October than at 60°N in March. This is probably because of the lower level of planetary wave activity in the southern hemisphere (see Chapter 2), which, in turn, is a consequence of the fact that there is much less land in the southern hemisphere. Losses of about 25 DU between the two time periods, at 60° in each hemisphere in winter, are also apparent. The most dramatic change is south of 75°S in October, where the development of the Antarctic ozone hole can be seen clearly.

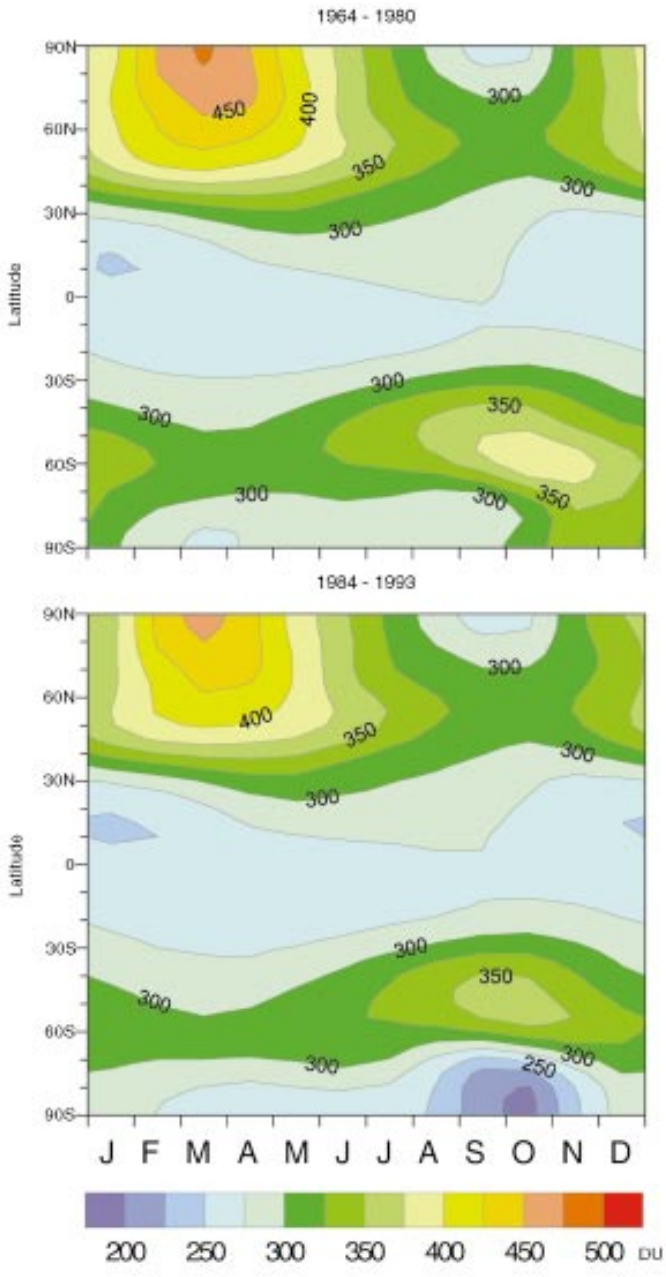

Figure 1.12 Mean total ozone (DU) as a function of latitude and season for 1964–1980 and 1984–1993. (Updated from Bojkov and Fioletov [1995].)

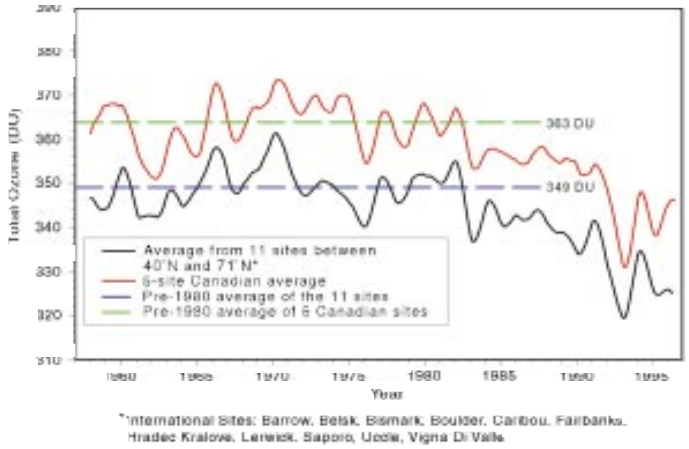

Figure 1.13 Total ozone over 5 Canadian stations and over 11 other midlatitude sites (smoothed, 1-year triangular filter).

Ozone decline over midlatitudes is much weaker than in the Antarctic, although it can be clearly seen from the long-term data records. Figure 1.13 shows the medium- and long-term variation of total ozone over Canada, compared with that of other northern midlatitude sites. The upper curve represents the average of daily total ozone measurements at the five Canadian stations (adjusted in the 1957–1964 period for the fact that not all stations were then operating), the lower curve the average of measurements from the other stations. In each case the smoothed seasonal variation (e.g., the solid curve in Figure 1.8) has been subtracted from the individual daily values, and then the remainder has been smoothed with a 365-day full-width half-maximum triangular filter[2] [Kerr 1991].

The two curves are similar, both in the overall trend and in their variation at time scales of two to five years. The natural year-to-year variation (as evidenced by the values prior to 1980) is of the order of a few percent. The fact that total ozone values are systematically higher over Canada is a manifestation of latitudinal and longitudinal differences in the global ozone distribution. These differences are a result of persistent meteorological features, caused by differences in topography that affect the propagation of planetary waves (see Chapter 2). Both curves demonstrate a decline in total ozone values by about 6% since the late 1970s. Similar trends are seen at other midlatitude stations and from space. In the equatorial belt there are no significant ozone changes [WMO 1994], although a temporary 2–3% total ozone decline is evident after the Mount Pinatubo eruption [e.g., Chandra 1993] .

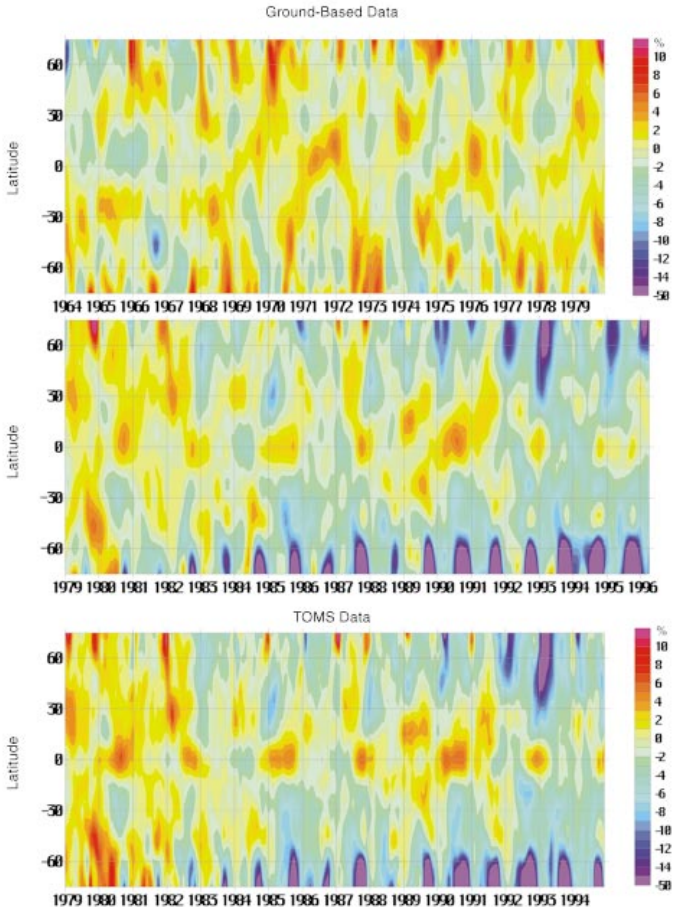

Figure 1.14 Latitude-time cross-section of deviations (%) in total ozone from the long-term mean, 1964–1980. (After Bojkov and Fioletov [1995].)

Figure 1.14 shows total ozone deviations from the long-term (1964–1980) mean, for the periods 1964–1979 and 1979–1996, calculated from ground-based and TOMS data. Both systems show a similar picture of ozone decline during the last 15–20 years. Very significant losses (>30%) are seen in the south polar region after 1980. Losses in the Arctic are smaller than in the Antarctic: typically about 12% in the winter-spring column ozone [Bojkov et al. 1995; McPeters et al. 1996]. This difference is known to be associated with the differences between the Arctic stratosphere vortex and the Antarctic stratosphere vortex [Manney and Zurek 1993]. In the Antarctic, the vortex and the cold temperatures within it persist longer into spring than is the case with the less circular and generally weaker and warmer Arctic vortex. The combination of low temperature (<–80°C) and sunlight, which allows rapid destruction of ozone, occurs to a much greater extent in Antarctica than in the Arctic.

Except in 1993, losses have been smaller (4–6%) at midlatitudes, but a clear downward trend is visible after about 1980. In the tropics the effect of the QBO can be clearly seen. Following the record ozone lows in the northern hemisphere winter of 1992–1993, values closer to normal are seen in 1994. Large negative ozone deviations are visible again in the 1994–1995 winter over northern tropical, middle, and high latitude areas. In the winter of 1995–1996 large negative deviations can be seen over northern high latitudes but not at middle latitudes. One may also see that deviations during the 1960s and 1970s are less significant, and do not show the dramatic trends of the 1980s and 1990s.

Figure 1.15 shows deviations from the long-term (1966–1987) means of vertical ozone distribution over Canada. The data are from weekly ozonesonde flights at the six Canadian stations. Deviations are in DU km^{-1}. The data have been smoothed by a 3-month running mean (boxcar filter). The pattern of low total ozone values during recent years is evident, and from these data it is also apparent that the major losses are in the lower stratosphere. Similar patterns can be seen in sonde data from Asia (Japan) and Europe (Figure 1.20).

Although ozone decline at midlatitudes was anticipated, the fact that the major losses have occurred in the lower stratosphere was surprising, since atmospheric ozone chemistry models employing gas phase reactions with chlorine (see Chapter 3) predict, at most, a decline of about 1% in total ozone since 1980 [Brasseur 1992; McElroy et al. 1992]. Additionally, the bulk of this decline was predicted by those models to occur in the upper stratosphere, near 40 km. Since midlatitude stratospheric temperatures are too warm to permit the formation of Polar Stratospheric Clouds (PSCs, see Chapter 3), the low temperature heterogeneous chemistry responsible for the Antarctic ozone hole cannot occur there. Contributing factors to the midlatitude loss are destruction via heterogeneous reactions on sulphate aerosols injected into the stratosphere from several large volcanic eruptions in the past decade [WMO 1991, 1994]; destruction via heterogeneous

[2] Each point on the smoothed curve is therefore a weighted average of the (deseasonalized) original data: i.e., if S_i and R_i are the values of the smoothed curve and the deseasonalized raw data respectively at day i, then

$$S_i = \frac{\sum_{n=-730}^{730} R_{i+n} \cdot W_n}{\sum_{n=-730}^{730} W_n}, \quad W_n = \frac{730-|n|}{730}, \quad \text{if } R_{i+n} \text{ exists,}$$
$$= 0, \quad \text{otherwise.}$$

This has the effect of suppressing short-term variations.

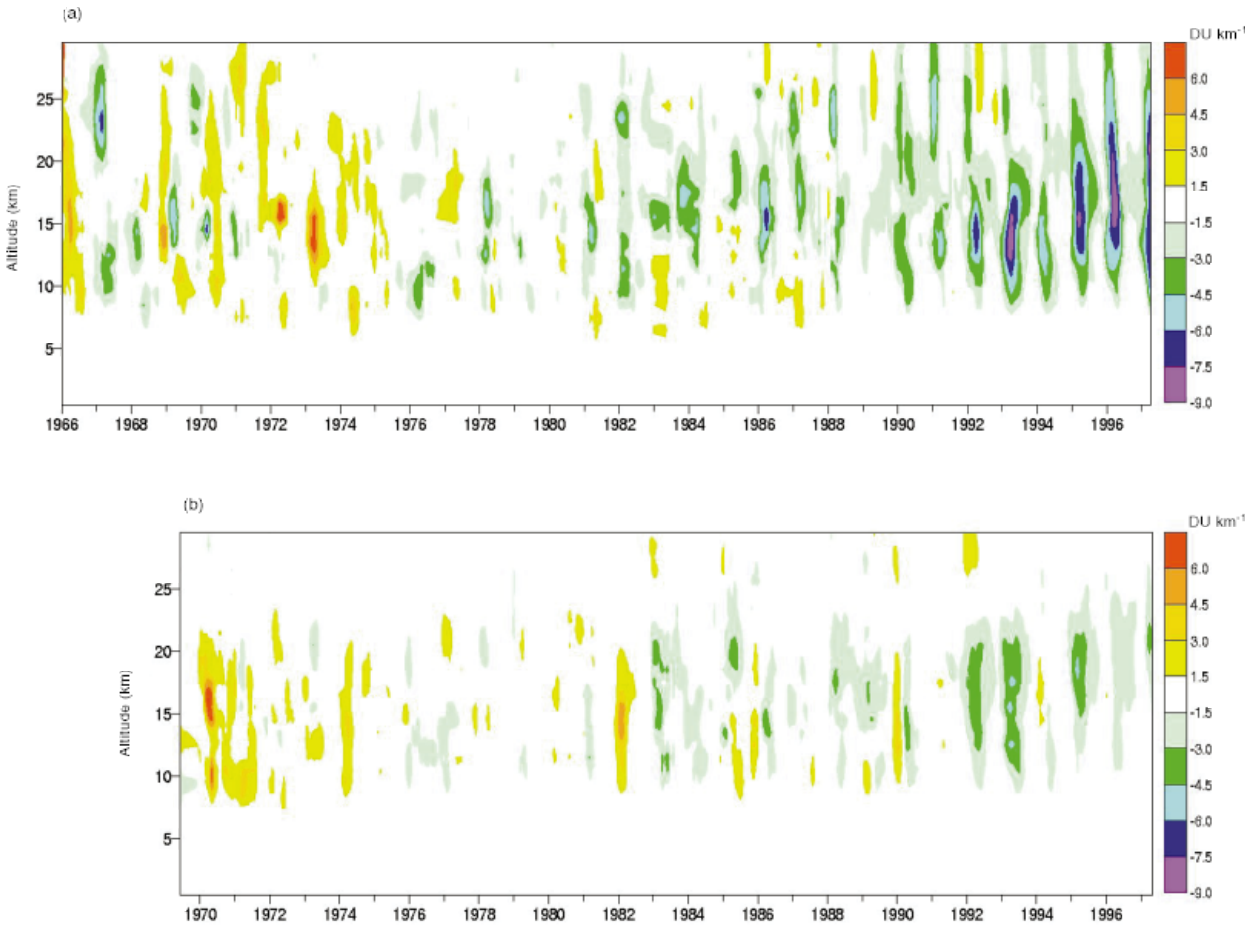

Figure 1.15 Deviations from the 1966–1987 means of ozone in DU km^{-1} over (a) Canadian Arctic stations (Resolute, Eureka, and Alert) and (b) Canadian midlatitude sites (Edmonton, Goose Bay, and Churchill). Values shown are 3-month running means.

reactions on PSCs in the Arctic winter stratosphere, with subsequent transport to lower latitudes; and possible changes in dynamics, such as the warming of the global troposphere. In addition, a possible side effect of global warming is a cooling of the Arctic stratosphere leading to an enhanced rate of ozone destruction by heterogeneous processes [Austin et al. 1992].

1.3.2 Recent Occurrences of Low Ozone Values

In 1992 and 1993 very low ozone values were observed almost everywhere from the equator to the poles [Gleason et al. 1993, Schoeberl et al. 1993, Chandra 1993, Kerr et al. 1993]. Over Canada the dramatic losses in the spring of 1993 were at that time the largest ever seen [Kerr et al. 1993]. Total ozone values were 10–17 % below normal, and the peak loss was 30% at 16 km. Record low average total ozone values for the period January–April were observed at three of the four midlatitude stations where measurements have been made since the 1960s. These extreme values were not seen in the spring of 1994, however, and the phenomenon is attributed to the effects (dynamical and/or chemical) of the eruption in the Philippines in June 1991 of Mt. Pinatubo, which injected more SO_2 into the stratosphere than any other volcano this century [Brasseur and Granier 1992; Labitzke and McCormick 1992; Schoeberl et al. 1993; Solomon et al. 1996].

In March of 1997 Canadian stations in the Arctic recorded large depletions in total column ozone relative to long-term station mean values. These losses, the largest ever seen in 40 years of ozone monitoring in the Canadian Arctic, exceeded the dramatic losses of 1993. Monthly mean ozone concentration values at 16 km were 40% lower than long-term means, and deviations in total ozone were more than 45% (4σ) for some individual days [Fioletov et al. 1997; Newman et al. 1997]. The net ozone loss was similar to that which occurred in recent years in the Antarctic, although the amount of ozone remaining is still much greater. (In 1997, ozone in the Arctic declined from an undisturbed value of 450 DU to below

300 DU, while in Antarctica values have typically declined from 300 DU to about 100 DU.) The low ozone values in the Arctic were associated with very low temperatures, apparently owing to a reduced eddy flux of heat into the polar vortex [Newman et al. 1997]. This may imply reduced transport of ozone as well. However, polar stratospheric clouds were observed frequently from the observatory at Eureka as were high values of chlorine monoxide in the first two weeks of March [Donovan et al. 1997; Santee et al. 1997]. This suggests that, as in the Antarctic spring, the low temperatures within the arctic stratosphere vortex led to the formation of PSCs, permitting the generation of chlorine monoxide, which in the presence of sunlight rapidly destroys ozone (see Chapter 3). There were also very cold temperatures and low ozone values during the February–March period of 1996.

Total ozone maps and maps of ozone deviations in percent for March 1993 and March 1997 are shown in Figure 1.16.

While the 1993 ozone loss was widespread over Canada, that of 1997, while much more pronounced in the Arctic, was not observed at midlatitudes. This may also be seen from Figure 1.15.

1.3.3 Total Ozone Trends

Figure 1.17 shows trends from a large number of ground-based total ozone measuring stations (Dobson and Brewer) located between 60°S and 60°N, and possessing good calibration histories. The station records are those used in the recent UNEP Assessment [WMO 1994], with the addition of data for 1995 and 1996. The Canadian stations with long-term records (Toronto, Edmonton, Goose, and Churchill) are indicated by solid circles. A regression model that allows for annual, QBO, and solar cycle variations and assumes a linear trend beginning in 1979 [Bojkov et al. 1995] was used to estimate trends.

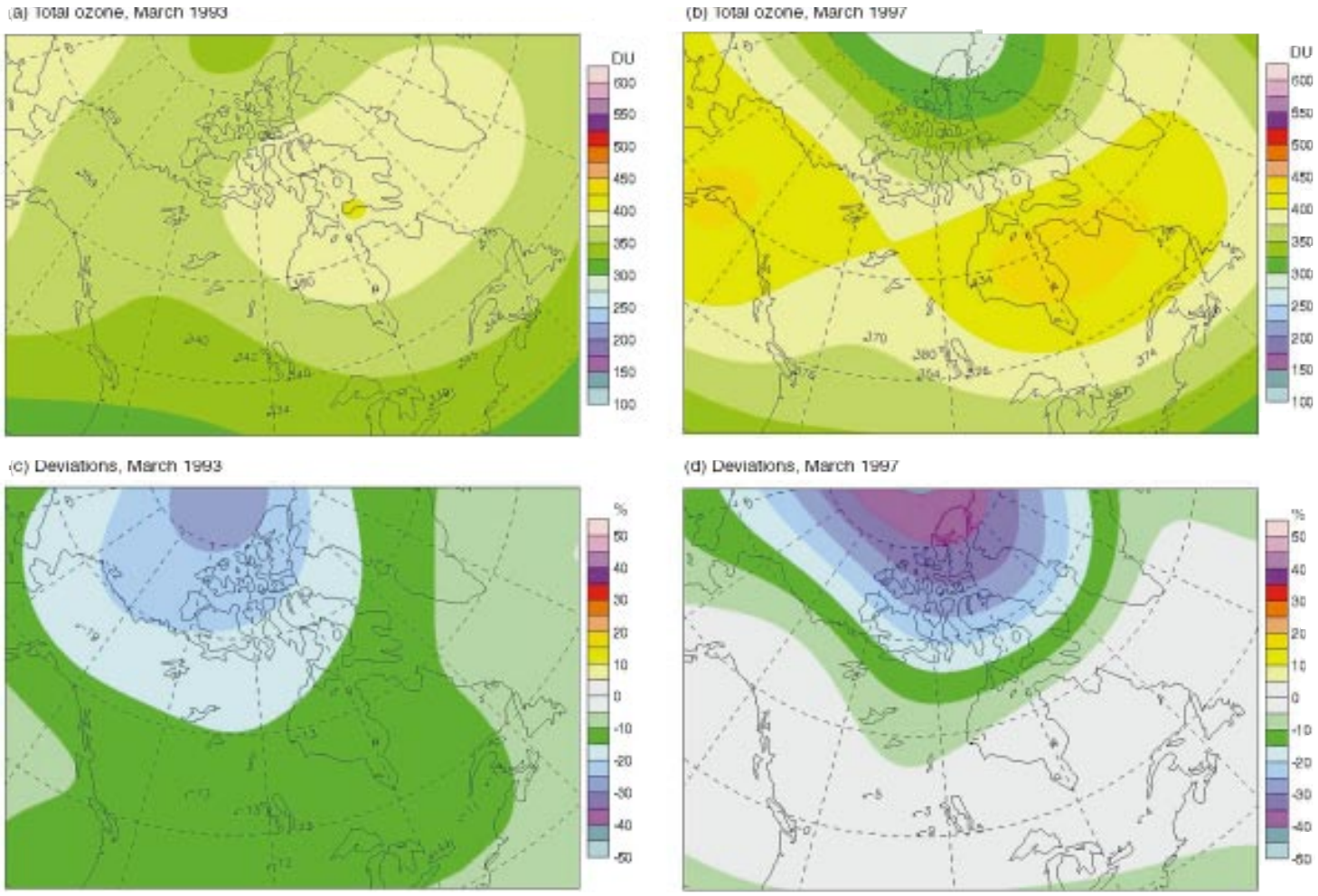

Figure 1.16 Total Ozone over Canada: (a, b): average values for March 1993 and March 1997; (c, d): percentage differences from the 1979–1988 average.

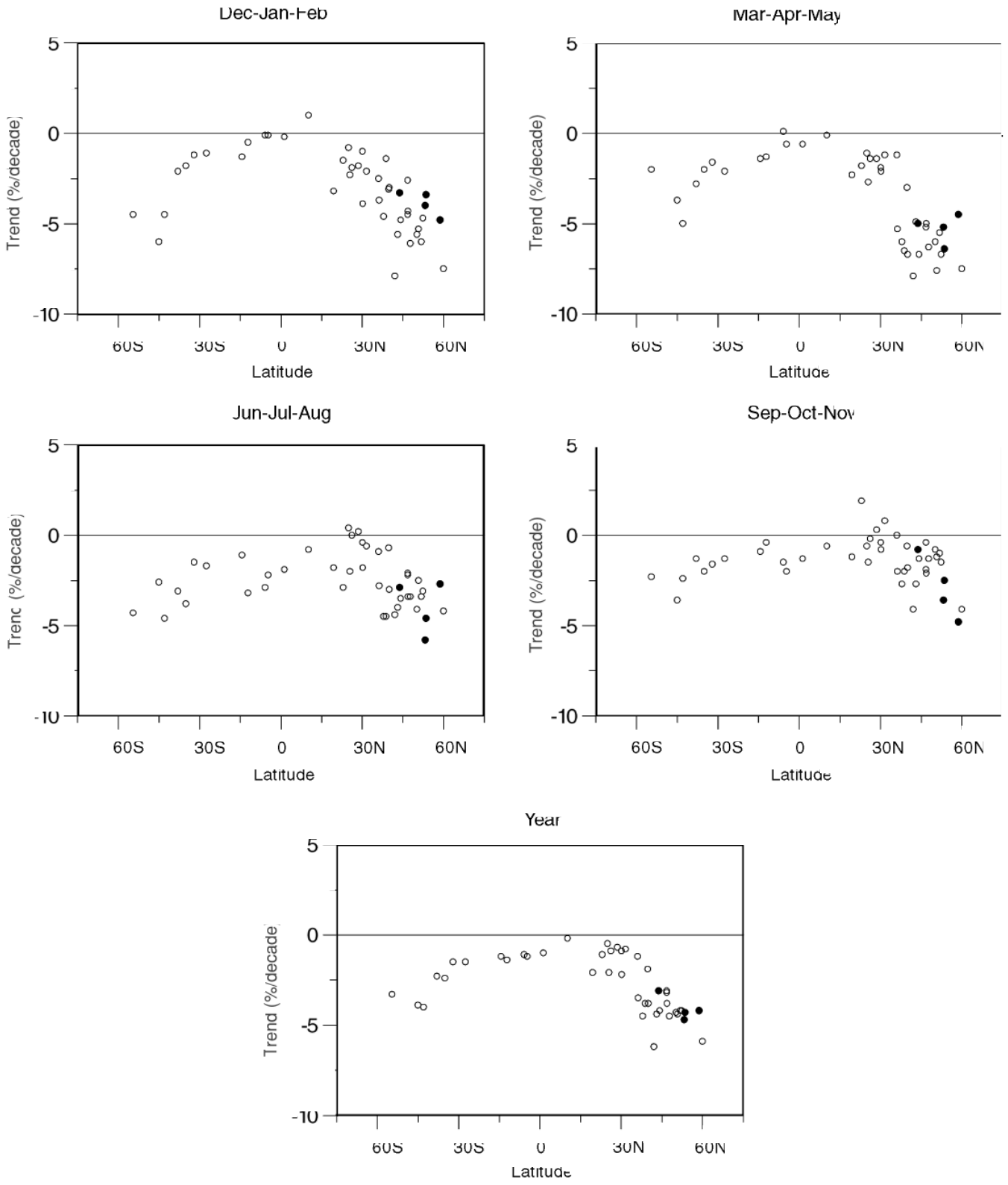

Figure 1.17 Decadal trends in annual and seasonal total ozone averages by latitude, from ground-based data.

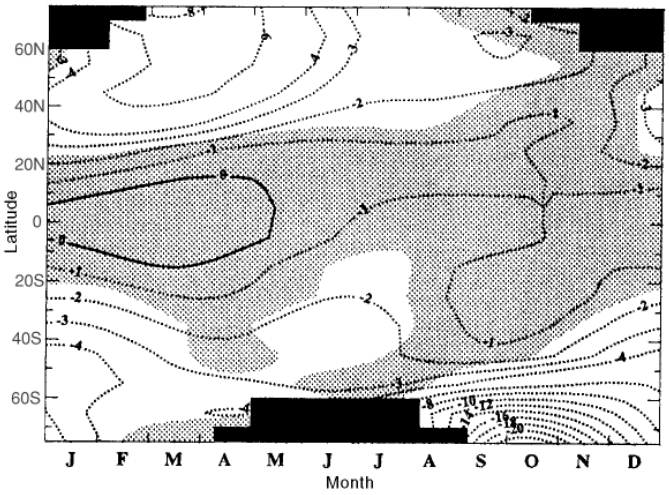

Figure 1.18 Trends in total ozone from TOMS (percentage change per decade), 1978–1994. (From McPeters et al. [1996].)

Examination of the station trends of Figure 1.17 and the satellite data of Figure 1.18 reveals the major latitude and seasonal trend patterns. Midlatitude trends are only slightly different in the two hemispheres. The annual average at 45°S is slightly less (about 4% vs 5% per decade), the seasonal variation is weaker, and the peak occurs later in relation to the spring equinox than at 45°N. The trends are largest poleward of 45°. The strongest decline, more than 20% per decade in the southern polar region during the austral spring, reflects the development of the Antarctic ozone hole.

Trends are not statistically significant between 20°N and 20°S. The tendency toward large negative springtime trends can also be seen in Figure 1.8; the recent measurements fall below the pre-1980 values primarily in the early part of the year. Since ozone is generally much higher at this time of year, these early springtime losses are less serious with respect to human UV exposure than would be summertime losses of similar magnitude. However, the reverse may be the case for aquatic ecosystems as well as crops and other vegetation, which may be more sensitive in the early spring (see Chapter 5).

Deseasonalized annual averages of total ozone for five Canadian stations with long-term records are shown in Figure 1.19 as a deviation in percent from the pre-1980 average. All data are direct-sun observations. No correction has been made for QBO, solar cycle, or other effects. Interannual variability of the order of ±5% is evident, as is the general decline in average ozone values from 1980 onwards. After 1982 the annual deviations are negative, with few exceptions, at all stations, and a tendency toward even lower values in the 1990s is apparent at all stations. The best-fit linear trend to the 1980–1996 data is shown, as well as the 95% confidence limits (dotted curves) for that trend. The trend is negative and statistically significant at the 95% confidence level at all stations.

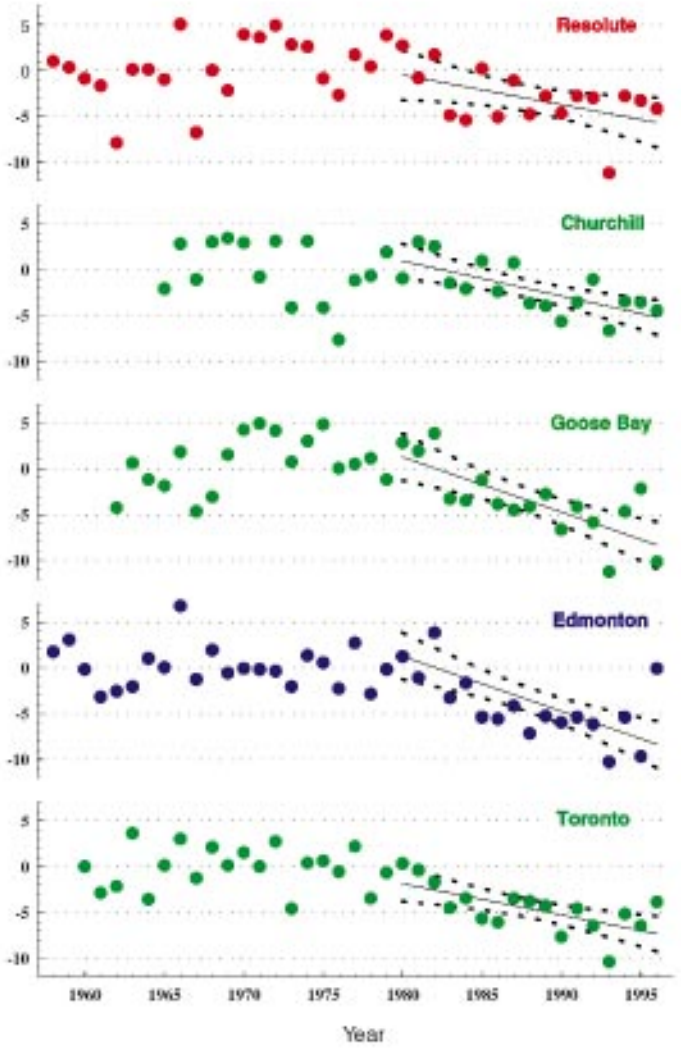

Figure 1.19 Trends in total ozone at Canadian stations. The trend toward lower values in the 1980s and 1990s is indicated. The calculated trends are all statistically significant at the 95% level.

1.3.4 Trends in the Vertical Distribution of Ozone

Figure 1.20 shows deviations from the long-term (1974–1988) means of vertical ozone distribution over Canada, Europe, and Japan. The data are from ozonesonde flights at Hohenpeissenberg and Lindenberg (Germany), Payerne (Switzerland), Churchill, Goose Bay, and Edmonton (Canada), and Sapporo and Tateno (Japan) [Bojkov and Fioletov 1997]. The annual cycle has been removed. Deviations are in ozone partial pressure (nanobars, or 10^{-6} hPa). The data have been smoothed by a 3-month running mean (boxcar filter). A high degree of variability is evident, but with few positive deviations and strong negative deviations after 1982 in all three regions. Most notable are the large negative deviations in 1993 (in all regions) and in 1995 (in Canada and Japan).

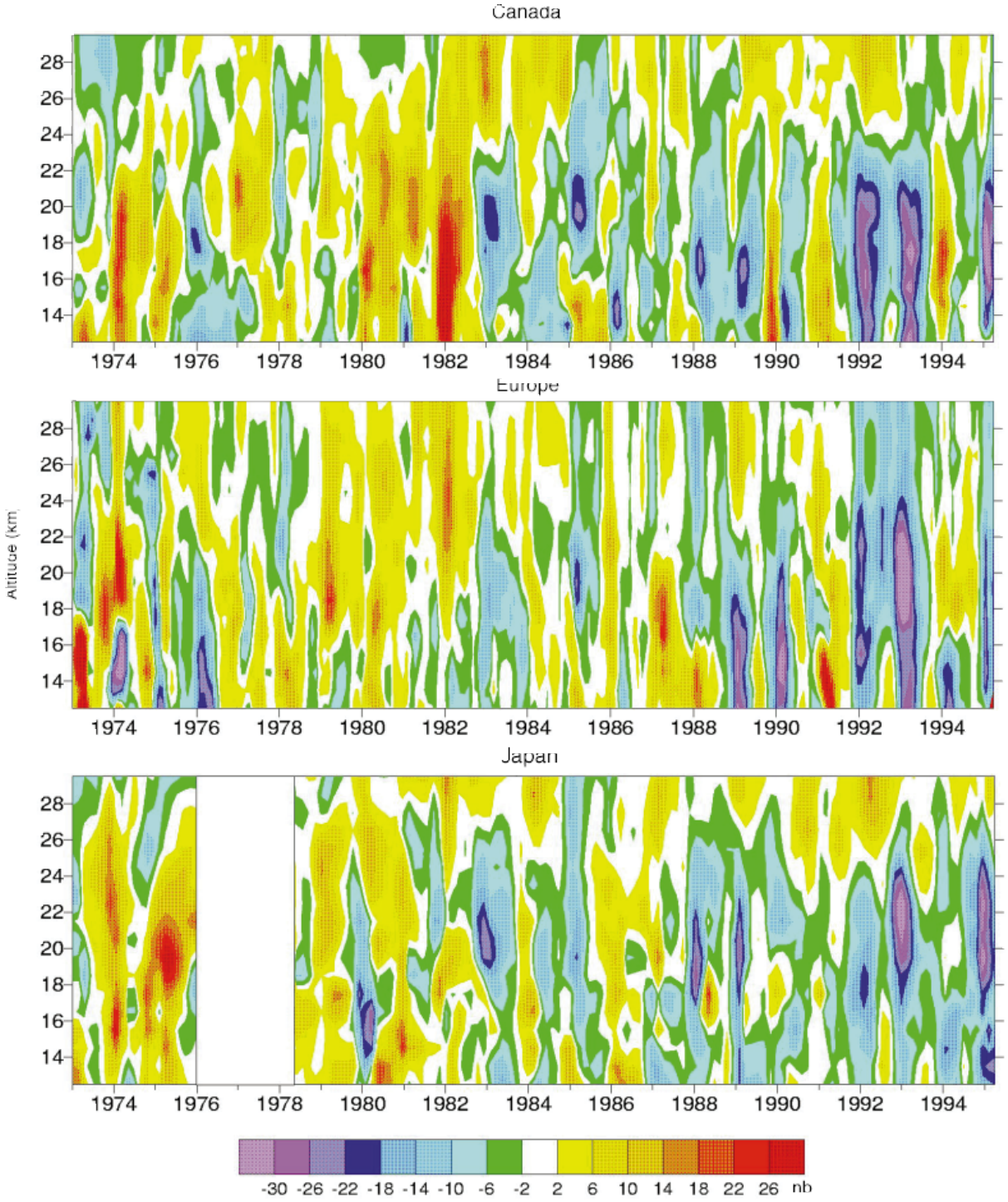

Figure 1.20 Ozone deviations from the long-term (1974–1988) means over Canada, Europe and Japan, expressed as ozone partial pressure (nanobars, or 10^{-6} hPa). The data have been smoothed by a 3-month running mean (boxcar filter). (From Bojkov and Fioletov [1997].)

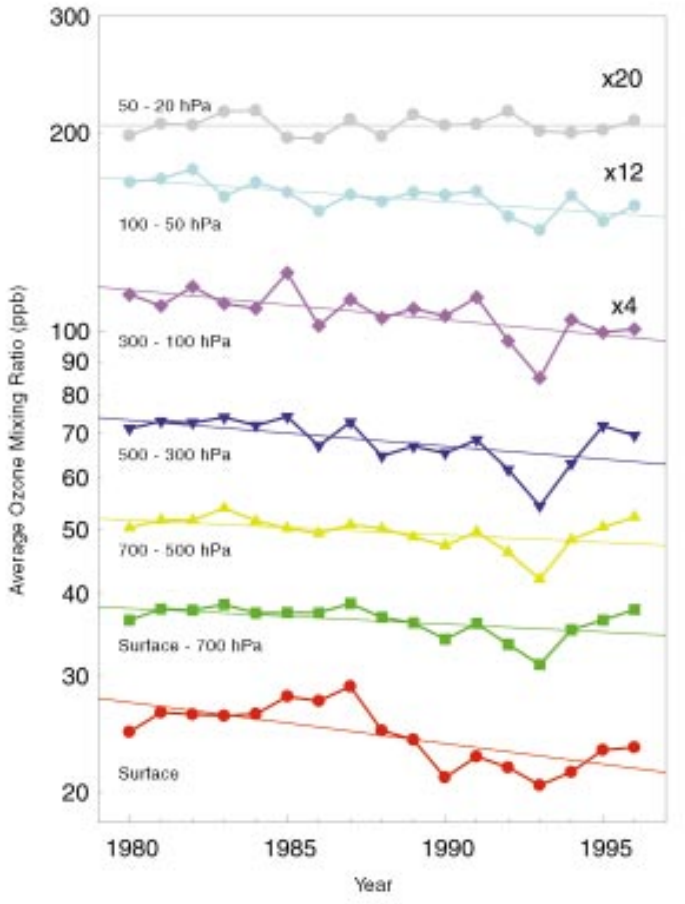

Figure 1.21 Trends in ozone mixing ratio over Canada (5-station average), from ECC ozonesonde data, 1980–1996. Data for Alert (1988–1996) have been included, after adjustment to the four-station mean for that period. Values for the top three plots should be multiplied by the indicated factors to get the correct mixing ratio.

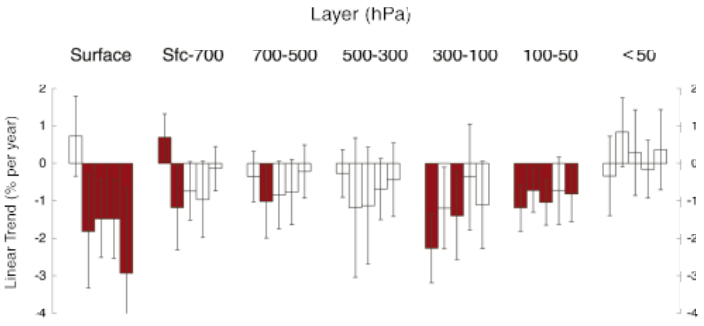

Figure 1.22 Trends in ozone mixing ratio at five Canadian sites, from ECC ozonesonde data, 1980–1996, for six layers and the surface. Stations in each group (left to right): Alert, Resolute, Churchill, Goose Bay, Edmonton. Trends significant at the 95% level are indicated by dark shading.

Figure 1.21 presents the average trends in ozone at different pressure heights over Canada. The atmosphere has been divided into six layers: surface–700 hPa, 700–500 hPa, 500–300 hPa, 300–100 hPa, 100–50 hPa, and 50–20 hPa. Annual average values of the ozone mixing ratio are shown for each layer. The lower two stratospheric layers show the expected decline, as seen throughout the northern hemisphere. The three tropospheric layers also show a similar decline. This behaviour is found at other North American sonde stations [Oltmans et al. 1997], but it contrasts with results from Europe and Japan [Oltmans et al. 1997; Claude et al. 1996; Logan 1994] that show similar negative trends in the stratosphere but positive trends up to the late 1980s in the troposphere.

The steady decrease of mixing ratio from the lower stratosphere to the surface is consistent with the hypothesis that stratospheric injection is a major source of tropospheric ozone in remote northern regions, as has been suggested by studies of tropopause folding using ozonesondes [Oltmans et al. 1989] and recent studies using aircraft [Bachmeier et al. 1994; Browell et al. 1994]. Comparison of the long-term trends is also suggestive: the three free tropospheric layers show essentially the same behaviour as the lower two stratospheric layers. Moreover, the year-to-year variations in all five layers show some correlation. In particular, the large losses in the lower stratosphere in 1993 [Kerr et al. 1993] and subsequent recovery are also reflected in similar losses and recoveries in all three tropospheric layers and possibly even at the surface. Other mechanisms than stratospheric injection have been suggested to explain this correlation in remote northern regions: one possibility is increased *destruction* of ozone in the upper troposphere by higher levels of UV-B radiation penetrating a reduced stratospheric layer [Taalas et al. 1997; Madronich and Granier 1994].

Figure 1.22 shows trends derived for the same atmospheric layers for each of five Canadian sonde stations. (Eureka has been omitted as the record is too short.) The sonde data were integrated within these layers to produce values for the partial ozone column in each layer, which were then converted to an average mixing ratio in parts per billion (ppb). The mixing ratio time series were deseasonalized, and then, as the sonde record is not entirely regular in time, they were binned by month. In order to avoid the effects of autocorrelation within the year on the error estimates of the derived trends, these monthly averages were further averaged into annual averages on which a simple linear regression was then used to derive trends.

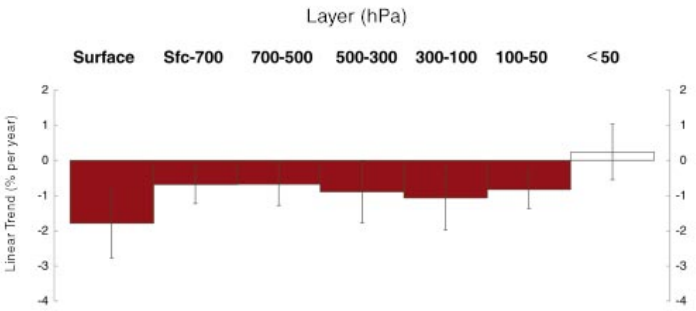

Figure 1.23 Trends in ozone mixing ratio averaged over the five Canadian stations. Data for Alert (1988–1996) have been included, after adjustment to the four-station mean for that period. Trends significant at the 95% level are indicated by dark shading.

Except for Alert at the surface and in Layer 1, all stations show primarily negative trends. The trends for the five-station average (Figure 1.23) are all negative in the troposphere, including the trends in surface ozone (derived from the measurements made by the sondes at the point of launch). All are statistically significant at the 2σ level. Overall, surface trends are nearly twice as large as those in the three free tropospheric layers [Tarasick et al. 1995, 1996b].

1.4 Forecasting Day-to-day Changes in Total Ozone

It has been known since the 1920s that total ozone variations are highly correlated with synoptic scale meteorological disturbances, particularly at extratropical latitudes [Dobson and Harrison 1926; Dobson et al. 1929, 1930, 1946]. Detailed examination of weather patterns and total ozone amounts reveals some simple relationships between them [Reed 1950; Vaughan and Price 1991; Wirth 1993]. For example, high total ozone is associated with an upper air trough, and low total ozone with a ridge, and ozone is observed to increase and decrease with the passage of cold and warm fronts respectively. Total ozone has been shown to be correlated with lower stratospheric temperatures, geopotential heights, and winds [Ohring and Muench 1959], with tropopause pressure (or height) [Schubert and Munteanu 1988], and with isentropic potential vorticity near the tropopause [Vaughan and Begum 1989; Allaart et al. 1993]. Knowledge of these relationships was the basis for the development of Environment Canada's Ozone/UV-B Forecast Model, which uses the output from the operational forecast model at the Canadian Meteorological Centre to forecast total ozone and thence UV-B (see Chapter 4). The ozone forecast model that became operational in 1993 [Burrows et al. 1995] is based on multiple regressions of historical values of total ozone and meteorological variables. The initial forecast produced by the regression equations is corrected, using knowledge of current ozone measurements at the 12 Canadian Brewer sites and their forecasted values from the previous day, to produce the final forecast. Figure 1.24 shows that, in general, the model has performed extremely well, with typical root mean square errors of only approximately 10 DU.

The model's good performance is in large part due to the simple correction procedure that it uses. Research is currently in progress to improve the stratospheric part of the Canadian Meteorological Centre's global forecast model and to include ozone as a model variable. A three-dimensional optimal data assimilation system (3DVAR) is also under development, along with the necessary algorithms to assimilate ozone data, both from satellite instruments such as GOME and from the Canadian ground-based network.

1.5 Trends in Ozone-Depleting Substances and Stratospheric Chlorine

The Montreal Protocol, which by mid-1997 had been signed by 163 countries, has established controls on the major ozone-depleting substances. Under the terms of the protocol and the subsequent London and Copenhagen amendments, the industrialized countries agreed to cease production of halons by the end of 1993 and of CFCs, carbon tetrachloride, and methyl chloroform by the end of 1995. Following meetings in Vienna (1995) and Costa Rica (1996), agreement was reached on gradual reductions in the use of methyl bromide and on its complete phase-out by 2010.

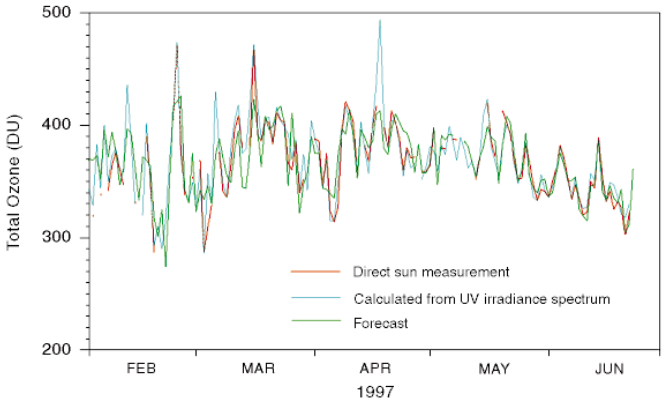

Figure 1.24 Ozone forecasts at Montreal: Total column ozone measured by Brewer at Montreal versus the ozone predicted by the forecast model at CMC.

Assuming that the Montreal Protocol provisions are obeyed, it is estimated that the amount of chlorine in the stratosphere, currently about 3.5 parts per billion, will peak within the next five years and that it will decrease thereafter. It should reach the 1980 level of 2.0 ppb by 2050 and the natural level of 1.0 ppb some time after 2100 [WMO 1991, 1994]. Uncertainties in the extent to which countries adhere to their obligations under the protocol as well as modelling uncertainties will no doubt cause these estimates to be revised many times before then.

Chlorine concentrations in the stratosphere follow those in the troposphere with a time lag of three to five years. Observations of tropospheric CFCs at Barrow and Alert are shown in Figure 1.25. CFC-11 and CFC-12 are destroyed in the atmosphere at a rate of about 2% and 1% per year respectively. The measurements for both show strong evidence of decreasing rates of emission into the atmosphere. In the case of CFC-11, the emission rate is now less than the destruction rate, and the concentration is therefore declining. With CFC-12, the rate of increase has been much reduced since about 1990. It is encouraging that tropospheric concentrations of these CFCs are already clearly showing the effects of the Montreal Protocol controls.

That ozone depletion has been caused by increasing chlorine and bromine amounts in the stratosphere is beyond doubt, and it is therefore reasonable to assume that ozone depletion should diminish as the chlorine and bromine content of the stratosphere declines. However, other factors such as different anthropogenic gases or possibly global warming may be significant contributors to ozone depletion. Current models do not reproduce observed ozone depletion well enough to rule out a contribution from these factors. Thus, stratospheric chlorine or bromine or any combination of these is a proxy for ozone depletion but not necessarily an accurate or complete one. Also, because there is a much greater variability in ozone than stratospheric chlorine, any recovery in ozone will take many more years to detect than a corresponding one in the chlorine values.

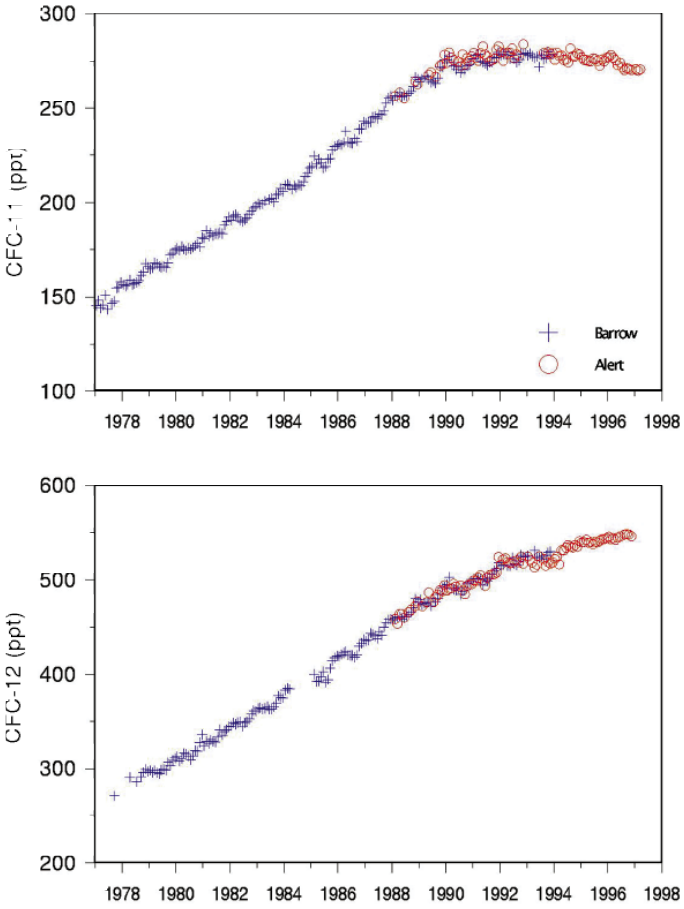

Figure 1.25 Measurements of tropospheric CFC concentration, from flask samples taken at Alert, N.W.T., and Barrow, Alaska. (Courtesy J.W. Elkins, NOAA.)

References

Allaart, M.A., H. Kelder, and L.C. Heijboer, 1993. On the relation between ozone and potential vorticity. *Geophys. Res. Lett*., **20**, 811–814.

Anderson, J.G., W.H. Brune, S.A. Lloyd, D.W. Toohey, S.P. Sander, W.L. Starr, M. Loewenstein, and J.R. Podolske, 1989. Kinetics of O_3 destruction by ClO and BrO within the Antarctic vortex: An analysis based on in situ ER-2 data. *J. Geophys. Res.,* **94**, 9837–9846.

Angell, J. K., and J. Korshover, 1973. Quasi-biennial and long-term fluctuations in total ozone. *Mon. Weather Rev.,* **101**, 426–443.

Angell, J.K., and J. Korshover, 1976. Global analysis of recent total ozone fluctuations. *Mon. Weather Rev.,* **104**, 63–75

Austin J., N. Butchart, and K. P. Shine, 1992. Possibility of an Arctic ozone hole in a doubled-CO_2 climate. *Nature,* **360**, 221–225.

Bachmeier, E.V., M.C. Shipman, E.V. Browell, W.B. Grant, and J.M. Klassa, 1994. Stratospheric/tropospheric exchange affecting the northern wetlands regions of Canada during summer 1990. *J. Geophys. Res*., **99**, 1793–1804.

Bojkov, R.D., and V.E. Fioletov, 1995. Estimating the global ozone characteristics during the last 30 years. *J. Geophys. Res*., **100**, 16,537–16,551.

Bojkov, R. D., V.E. Fioletov, and A.M. Shalamjansky, 1994. Total ozone changes over Eurasia since 1973 based on reevaluated filter ozonometer data. *J. Geophys. Res.,* **99**, 22,985–22,999.

Bojkov R.D., L. Bishop and V.E. Fioletov, 1995. Total ozone trends from quality-controlled ground-based data (1964–1994). *J. Geophys. Res.,* **100**, 25,867–25,876.

Bojkov, R.D., and V.E. Fioletov, 1997. Changes of the lower stratospheric ozone over Europe and Canada. *J. Geophys. Res.,* **102,** 1337-1347.

Bowman, K.P., 1989. Global patterns of the quasi-biennial oscillation in total ozone. *J. Geophys. Res.,* **99**, 3328–3343.

Bowman, K.P. and A.J. Krueger, 1985. A global climatology of total ozone from the Nimbus-7 Total Ozone Mapping Spectrometer (TOMS). *J. Geophys. Res.*, **90**, 9767–9776.

Brasseur, G.P., 1992. Natural and anthropogenic perturbations of the stratospheric ozone layer. *Planet. Space Sci*., **40**, 403–412.

Brasseur, G., and C. Granier, 1992. Mount Pinatubo aerosols, chlorofluorocarbons, and ozone depletion. *Science,* **257**, 1239–1242.

Brewer, A.W., 1949. Evidence for a world circulation provided by the measurements of helium and water vapour distribution in the stratosphere. *Quart. J. R. Met. Soc*., **75**, 351–363.

Brewer, A.W., and J.R. Milford, 1960. The Oxford-Kew sonde. *Proc. Roy. Soc. A,* **256**, 470–495.

Browell, E.V., M.A. Fenn, C.F. Butler, W.B. Grant, R.C. Harriss, and M.C. Shipman, 1994. Ozone and aerosol distributions in the summertime troposphere over Canada. *J. Geophys. Res.,* **99**, 1739–1755.

Brune, W.H., J.G. Anderson, and K.R. Chan, 1989. In situ observations of ClO in the Antarctic: ER-2 aircraft results from 54° to 72°N latitude. *J. Geophys. Res.,* **94**, 16649–16663.

Brune, W.H., D.W. Toohey, J.G. Anderson, and K.R. Chan, 1990. In situ observations of ClO in the arctic stratosphere: ER-2 aircraft results from 59° to 80°N latitude. *Geophys. Res. Lett.,* **17**, 505–508

Burrows, W., M. Vallee, D.I. Wardle, J.B. Kerr, L.J. Wilson, and D.W. Tarasick, 1995. The Canadian UV-B and Total Ozone Forecast Model. *Met. Apps.,* **1**, 247-265.

Chandra, S., 1991. The solar UV–related changes in total ozone from a solar rotation to a solar cycle. *Geophys. Res. Lett.*, **18**, 837–840.

Chandra, S., 1993. Changes in stratospheric ozone and temperature due to the eruptions of Mt. Pinatubo. *Geophys. Res. Lett.,* **20**, 33–36.

Chandra, S., and R.S. Stolarski, 1991. Recent trends in stratospheric total ozone: Implications of dynamical and El Chichon perturbations. *Geophys. Res. Lett.,* **18**, 2277–2280.

Chandra, S., and R.D. McPeters, 1994. The solar cycle variation of ozone in the stratosphere inferred from Nimbus 7 and NOAA 11 satellites. *J. Geophys. Res*, **99**, 20665–20671.

Claude, H., U. Kohler, and W. Steinbrecht, 1996. New trend analyses of the homogenized total ozone records at Hohenpeissenberg. *Proc. Quad. Ozone Symp.,* L'Aquila, Italy, 12–21 September, 1996, in press.

Danielson, E.F., 1983. Ozone Transport. Pages 161–194 in *Ozone in the Free Atmosphere.* R.C. Whitten and S.S. Prasad, eds. Princeton: Van Nostrand Reinhold.

Deluisi, J.J., D.U. Longnecker, C.L. Mateer, and D.J. Wuebbles, 1989. An analysis of northern middle-latitude Umkehr measurements corrected for stratospheric aerosols for 1979–1986. *J. Geophys. Res.,* **94**, 9837–9846.

Dobson, G.M.B., and D.N. Harrison, 1926. Measurements of the amount of ozone in the earth's atmosphere and its relation to other geophysical conditions: Part I. *Proc. Roy. Soc. London,* **A110**, 660–693.

Dobson, G.M.B., D.N. Harrison, and J. Lawrence, 1929. Measurement of the amount of ozone in the earth's atmosphere and its relation to other geophysical conditions: Part III. *Proc. Roy. Soc. London*, **A122**, 456–486.

Dobson, G.M.B., H.H. Kimball, and E. Kidson, 1930. Measurement of the amount of ozone in the earth's atmosphere and its relation to other geophysical conditions, Part IV. *Proc. Roy. Soc. London*, **A129**, 411–433.

Dobson, G.M.B., A.W. Brewer, and B.M. Cwilong, 1946. Meteorology of the lower stratosphere. *Proc. Roy. Soc. London*, **A185**, 144–175.

Donovan, D.P., J.C. Bird, J.A. Whiteway, T.J. Duck, S.R. Pal, A.I. Carswell, J.W. Sandilands, and J.W. Kaminski, 1996. Ozone and aerosol observed by lidar in the Canadian Arctic during the winter of 1995/96. *Geophys. Res. Lett.,* **23**, 3317–3320.

Donovan, D. P., H. Fast, Y. Makino, J.A. Whiteway, J.W. Kaminski, V. Savastiouk, J.C. Bird, A.I. Carswell, J. Davies, T.J. Duck, C.T. McElroy, R.L. Mittermeier, S.R. Pal, and D. Velkov,1997. Ozone, chlorine oxide, and polar stratospheric clouds observed over the NDSC observatory at Eureka during spring 1997. *Geophys. Res. Lett.,* **24**, in press.

Evans, W.F.J., J.B. Kerr, C.T. McElroy, R.S. O'Brien, B.A. Ridley, and D.I. Wardle, 1977. The odd nitrogen mixing ratio in the stratosphere. *Geophys. Res. Lett.,* **4**, 235–238.

Evans, W.F.J., J.B. Kerr, C.T. McElroy, R.S. O'Brien, and J.C. McConnell, 1982. Measurement of NO_2 and HNO_3 during a stratospheric warming at 54^{o}N in February 1979. *Geophys. Res. Lett.,* **9**, 493–496.

Evans, W.F.J., C.T. McElroy, and I.E. Galbally, 1985. The conversion of N_2O_5 to HNO_3 at high latitudes in winter. *Geophys. Res. Lett.,* **12**, 825–828.

Farman, J.C., B.G. Gardiner and J.D. Shanklin, 1985. Large losses of ozone in Antarctica reveal seasonal ClO_x/NO_x interaction. *Nature,* **315**, 207–210.

Fisher, M., and D.J. Lary, 1995. Lagrangian four-dimensional variational data assimilation of chemical species. *Quart. J. R. Met. Soc.,* **121**, No. 527 Part A, 1681–1704.

Fioletov, V.E., 1993. Total ozone "normal" values and mapping algorithm used in the atlas. Pages 17–28 in *Atlas of GO$_3$OS total ozone maps for the northern hemisphere winter-spring of 1992–1993.* WMO Ozone Rep. 34. Geneva: World Meteorological Organization.

Fioletov, V.E., J.B. Kerr, D.I. Wardle, J. Davies, E.W. Hare, C.T. McElroy and D.W. Tarasick, 1997. Long-term decline of ozone over the Canadian Arctic to early 1997 from ground-based and balloon sonde measurements. *Geophys. Res. Lett.,* **24**, in press.

Gleason, J. F., P. K. Bhartia, J. R. Herman, R. McPeters, P. Newman, R. S. Stolarski, L. Flynn, G. Labow, D. Larko, C. Seftor, C. Wellemeyer, W. D. Komhyr, A. J. Miller, and W. Planet, 1993. Record low global ozone in 1992. *Science,* **260**, 523–526.

Götz, F.W.P., A.R. Meetham, and G.M.B. Dobson, 1934. The vertical distribution of ozone in the atmosphere. *Proc. Roy. Soc. London*, **A145**, 416–446.

Gray, L.J., and S. Ruth, 1993. The modeled latitudinal distribution of the ozone quasi-biennial oscillation using observed equatorial winds. *J. Atmos. Sci.,* **50**, 1033–1046.

Hahn, J.F., C.T. McElroy, E.W. Hare, W. Steinbrecht, and A.I. Carswell, 1995. Intercomparison of Umkehr and differential absorption lidar stratospheric ozone measurements. *J. Geophys. Res.*, **100**, 25899–25911.

Hamilton. K., 1989. Interhemispheric asymmetry and annual synchronization of the ozone quasi-biennial oscillation. *J. Atmos. Sci.,* **46**, 1019–1025.

Herman, J. R., and D. Larko, 1994. Low ozone amount during 1992–1993 from Nimbus 7 and Meteor 3 total ozone mapping spectrometers. *J. Geophys. Res.*, **99**, 3483–3496.

Hasebe, F., 1983. Interannual variations of global ozone revealed from NIMBUS 4 BUV and ground-based observations. *J. Geophys. Res*., **88**, 6819–6834.

Hasebe, F., 1994. Quasi-biennial oscillations of ozone and diabatic circulation in the equatorial stratosphere. *J. Atmos. Sci.,* **55**, 729–745.

Hilsenrath, E., W. Attmannspacher, A. Bass, W. Evans, R. Hagemeyer, R.A. Barnes, W. Komhyr, K. Mauersberger, J. Mentall, M. Proffitt, D. Robbins, S. Taylor, A. Torres and E. Weinstock, 1986. Results from the balloon intercomparison campaign (BOIC). *J. Geophys. Res.,* **91**, 13137–13152.

Hofmann, D.J., and S. Solomon, 1989. Ozone destruction through heterogeneous chemistry following the eruption of El Chichon. *J. Geophys. Res.,* **94**, 5029–5041.

Huang, T.Y.W., and G.P. Brasseur, 1993. Effect of long-term solar variability in a two-dimensional interactive model of the middle atmosphere. *J. Geophys. Res*, **98**, 20413–20427.

Kerr, J. B., 1991. Trends in total ozone at Toronto between 1960 and 1991. *J. Geophys. Res.,* **96**, 20703–20709.

Kerr, J.B., I. A. Asbridge, and W.F.J. Evans, 1988. Intercomparison of ozone measured by Brewer and Dobson spectrophotometers at Toronto. *J. Geophys. Res,* **93**, 11129–11140.

Kerr, J.B., D.I. Wardle, and D.W. Tarasick, 1993. Record low ozone values over Canada in early 1993. *Geophys. Res. Lett*., **20**, 1979–1982.

Komhyr, W.D., 1969. Electrochemical concentration cells for gas analysis. *Ann. Géophys.,* **25**, 203–210.

Labitzke, K., and M.P. McCormick, 1992. Stratospheric temperature increases due to Pinatubo aerosols. *Geophys. Res. Lett*., **19**, 207–210.

Lait, L.R., M.R. Schoeberl, and P.A. Newman, 1989. Quasi-biennial modulation of the Antarctic ozone depletion. *J. Geophys. Res.,* **94**, 11559–11571.

Levelt, P.F., M.A.F. Allaart, and H.M. Kelder, 1996. On the assimilation of total-ozone satellite data. *Ann. Géophys.,* **14**, 1111–1118.

Logan, J.A., 1994. Trends in the vertical distribution of ozone: an analysis of ozonesonde data. *J. Geophys. Res.,* **99**, 25553–25585.

London, J., R. D. Bojkov, S. Oltmans, and J. I. Kelly, 1976. *Atlas of the global distribution of total ozone, July 1957–June 1967,* NCAR Tech. Note/TN/113 STR, Boulder, Colorado: National Center for Atmospheric Research.

Madronich, S., and C. Granier, 1994. Tropospheric chemistry changes due to increased UV-B radiation. Pages 3–10 in *Stratospheric Ozone Depletion/UV-B Radiation in the Biosphere.* NATO ASI Series I18. R.H. Biggs and M.E.B. Joyner, eds. Berlin: Springer-Verlag.

Manney, G. L., and R. W. Zurek, 1993. Interhemispheric comparison of the development of the stratospheric polar vortex during the fall: A 3-dimensional perspective for 1991–1992. *Geophys. Res. Lett.,* **20**, 1275–1278.

Mateer, C.L., and J.J. Deluisi, 1992. A new Umkehr inversion algorithm. *J. Atmos. Terr. Phys.*, **54**, 537–556.

Mateer, C.L., and H.U. Dutsch, 1964. *Uniform Evaluation of Observations From the World Ozone Network.* Boulder, Colorado: National Center for Atmospheric Research.

McElroy, C.T., 1995. A spectrometer for the measurement of direct and scattered solar irradiance from on-board the NASA ER-2 high-altitude research aircraft. *Geophys. Res. Lett.,* **22**, 1361–1364.

McElroy, C.T., and J.B. Kerr, 1995. Table Mountain ozone intercomparison: Brewer ozone spectrophotometer Umkehr observations. *J. Geophys. Res.*, **100**, 9293–9300.

McElroy, M.B., R.J. Salawitch and K. Minschwaner, 1992. The changing stratosphere. *Planet. Space Sci.,* **40,** 373–401.

McElroy, C.T., C. Midwinter, D.V. Barton, and R.B Hall, 1995. A comparison of J-values from the compostion and photodissociative flux measurement with model calculations. *Geophys. Res. Lett.,* **22**, 1365–1368.

McElroy, C.T., J.F. Hahn, and E.W. Hare, 1997. Determining high-altitude trends in ozone from Brewer Umkehr observations made at Canadian stations. *Proc. Quad. Ozone Symp.,* L'Aquila, Italy, 12–21 September 1996, in press.

McPeters, R. D., and G.J. Labow, 1996. An assessment of the accuracy of 14.5 years of Nimbus 7 TOMS Version 7 ozone data by comparison with the Dobson network. *Geophys. Res. Lett.,* **23**, 3695–3698.

McPeters, R. D., S. M. Hollandsworth, L. E. Flynn, J R. Herman, and C. J. Seftor, 1996. Long-term ozone trends derived from the 16-year combined Nimbus 7/Meteor 3 TOMS Version 7 record, *Geophys. Res. Lett.,* **23**, 3699–3702.

Michelangeli, D.V., M. Allen, and Y.L. Yung, 1989. El Chichon volcanic aerosols: impact of radiative, thermal, and chemical perturbations. *J. Geophys. Res.,* **94**, 18429–18443.

NASA, 1992. *The Atmospheric Effects of Stratospheric Aircraft: A First Program Report*. NASA Reference Publication 1272. Washington, D.C.: National Aeronautics and Space Administration.

NASA, 1993. *The Atmospheric Effects of Stratospheric Aircraft: A Second Program Report.* NASA Reference Publication 1293. Washington, D.C.: National Aeronautics and Space Administration.

NASA, 1996. "1996 Antarctic Ozone Hole Below Record Size," *NASA HQ Public Affairs Office Press Release,* October 25, 1996. Washington, D.C.: National Aeronautics and Space Administration.

Newman P. A., J. F. Gleason, and R. S. Stolarski, 1997. Anomalously low ozone over the Arctic. *Geophys. Res. Lett.,* **24**, in press.

Oltmans, S.J., W.E. Raatz, and W.D. Komhyr, 1989. On the transfer of stratospheric ozone into the troposphere near the north pole. *J. Atmos. Chem*., **9**, 245–253.

Oltmans, S.J., A.S. Lefohn, H.E. Scheel, J.A. Harris, H. Levy II, I.E. Galbally, E-G. Brunke, C.P. Meyer, J.A. Lathrop, B.J. Johnson, D.S. Shadwick, E. Cuevas, F.J. Schmidlin, D.W. Tarasick, J.B. Kerr, and O. Uchino, 1997. Trends of ozone in the troposphere. *Geophys. Res. Lett.,* forthcoming.

Ohring, G., and H.S. Muench, 1959. Relationships between ozone and meteorological parameters in the lower stratosphere. *J. Meteor.*, **17**, 195–206.

Prather, M., 1992. Catastrophic loss of stratospheric ozone in dense volcanic clouds. *J. Geophys. Res.,* **97**, 10187–10191.

Randel, W. J., and J.B. Cobb, 1994. Coherent variations of monthly mean total ozone and lower stratosphere temperatures. *J. Geophys. Res.,* **99**, 5433–5474.

Randel, W. J., and F. Wu, 1995. *Climatology of stratospheric ozone based on SBUV and SBUV/2 data:1978-1994*, NCAR Technical Note NCAR/TN-412+STR. Boulder, Colorado: National Center for Atmospheric Research.

Reed, R.J., 1950. The role of vertical motion in ozone-weather relationships. *J. Meteor*., **7**, 263–267.

Reinsel, G.C., G.C. Tiao, A.J. Miller, D.J. Wuebbles, P.S. Connell, C.L. Mateer and J.J. DeLuisi, 1987. Statistical analysis of total ozone and stratospheric Umkehr data for trends and solar cycle relationship. *J. Geophys. Res*., **92**, 2201–2209.

Reinsel, G. C., G.C. Tiao, D.J. Wuebbles, J.B. Kerr, A.J. Miller, R.M. Nagatani, L. Bishop, and L.H. Ying, 1994. Seasonal trend analysis of published ground-based and TOMS total ozone data through 1991. *J. Geophys. Res*., **99**, 5449–5464.

Santee, M. L., G. L. Manney, L. Froidevaux, R. W. Zurek, and J. W. Waters, 1997. MLS observations of ClO and HNO_3 in the 1996–97 Arctic polar vortex. *Geophys. Res. Lett*., **24**, in press.

Schoeberl, M.R., P.K. Bhartia, and E. Hilsenrath, 1993. Tropical ozone loss following the eruption of Mt. Pinatubo. *Geophys. Res. Lett*., **20**, 29–32.

Schubert, S.D., and M.J. Munteanu, 1988. An analysis of tropopause pressure and total ozone correlations. *Mon. Weather Rev*., **116**, 569–582.

Shiotani, M., 1992. Annual, quasi-biannual, and El Nino-Southern Oscillation (ENSO) time-scale variations in equatorial total ozone. *J. Geophys. Res.,* **97**, 7625–7633.

Shiotani, M. and F. Hasebe, 1994. Stratospheric ozone variations in the equatorial region as seen in Stratospheric Aerosol and Gas Experiment Data. *J. Geophys. Res.,* **99**, 14575–14584.

Solomon S., R.W.Portmann, R.R. Garcia, L.W. Thomason, L.R. Poole, and M.P. McCormick, 1996. The role of aerosol variations in anthropogenic ozone depletion in the northern hemisphere. *J. Geophys. Res*, **101**, 6713–6727.

Stolarski, R., R. Bojkov, L. Bishop, C. Zerefos, J. Staehelin, and J. Zawodny, 1992. Measured trends in stratospheric ozone. *Science*, **256**, 343–349.

Stolarski, R., G.J. Labow, and R. D. McPeters, 1997. Springtime Antarctic total ozone measurements in the early 1970s from the BUV instrument on Nimbus 4. *Geophys. Res. Lett,* **24**, 591–594.

Taalas, P., J. Damski, E. Kyrö, M. Ginzburg, and G. Talamoni, 1997. Effect of stratospheric ozone variations on UV radiation and on tropospheric ozone at high latitudes. *J. Geophys. Res*., **102**, 1533–1539.

Tarasick, D.W., J.B. Kerr, D.I. Wardle, J.J. Bellefleur and J. Davies, 1995. Tropospheric ozone trends over Canada: 1980–1993. *Geophys. Res. Lett.,* **22,** 409–412.

Tarasick, D.W., G. Brunet, R. Daley, P. Gauthier, and W.E. Ward, 1996a. A Canadian middle atmosphere initiative, *Proc. Quad. Ozone Symp.,* L'Aquila, Italy, 12–21 September 1996, in press.

Tarasick, D.W., J.B. Kerr, D.I. Wardle, J.J. Bellefleur, S. Bunka and J. Davies, 1996b. Tropospheric ozone trends at Canadian stations: 1980–1995, *Proc. Quad. Ozone Symp.,* L'Aquila, Italy, 1996, in press.

Tie, X., G.P. Brasseur, B. Briegleb, and C. Granier, 1994. Two-dimensional simulation of Pinatubo aerosol and its effect on stratospheric ozone. *J. Geophys. Res*., **99**, 20545–20562.

Vaughan, G., and D.A. Begum, 1989. Correlation between ozone and potential vorticity. Pages 91–94 in *Ozone in the Atmosphere: Proceedings of the Quadrennial Ozone Symposium 1988*. R.D. Bojkov and P. Fabian, eds. Hampton, Virginia: Deepak.

Vaughan, G., and J.D. Price, 1991. On the relation between total ozone and meteorology. *Quart. J. R. Met. Soc.,* **117**, 1281–1298.

Wirth, V., 1993. Quasi-stationary planetary waves in total ozone and their correlation with lower stratospheric temperature. *J. Geophys. Res*., **98**, 8873–8882.

WMO, 1989. *Scientific Assessment of Stratospheric Ozone: 1989.* World Meteorological Organization Global Ozone Research and Monitoring Project, Report No. 20. Geneva: World Meteorological Organization.

WMO, 1991. *Scientific Assessment of Stratospheric Ozone: 1991.* World Meteorological Organization Global Ozone Research and Monitoring Project, Report No. 25. Geneva: World Meteorological Organization.

WMO, 1994. *Scientific Assessment of Stratospheric Ozone: 1994*. World Meteorological Organization Global Ozone Research and Monitoring Project, Report No. 37. Geneva: World Meteorological Organization.

Yang, H., and K.K. Tung, 1994. Statistical significance and pattern of extratropical QBO in column ozone. *Geophys. Res. Lett*., **21**, 2235–2238.

Zerefos, C. S., A.F. Bais, T.C. Ziomas, and R.D. Bojkov, 1992. On the relative importance of quasi-biennial oscillation and ENSO in the revised total ozone records. *J. Geophys. Res*., **97**, 10135–10144.